



HAL
open science

Cardiorespiratory alterations in a newborn ovine model of systemic viral inflammation

Stephanie Nault, Sophie Tremblay, Roqaya Imane, Sally Al-Omar, Charlene Nadeau, Nathalie Samson, Vincent Creuze, Guy Carrault, Patrick Pladys, Jean-Paul Praud

► To cite this version:

Stephanie Nault, Sophie Tremblay, Roqaya Imane, Sally Al-Omar, Charlene Nadeau, et al.. Cardiorespiratory alterations in a newborn ovine model of systemic viral inflammation. *Pediatric Research*, 2022, 92 (5), pp.1288-1298. 10.1038/s41390-022-01958-4. hal-03592516

HAL Id: hal-03592516

<https://hal.science/hal-03592516>

Submitted on 13 Apr 2022

HAL is a multi-disciplinary open access archive for the deposit and dissemination of scientific research documents, whether they are published or not. The documents may come from teaching and research institutions in France or abroad, or from public or private research centers.

L'archive ouverte pluridisciplinaire **HAL**, est destinée au dépôt et à la diffusion de documents scientifiques de niveau recherche, publiés ou non, émanant des établissements d'enseignement et de recherche français ou étrangers, des laboratoires publics ou privés.



Distributed under a Creative Commons Attribution - NonCommercial 4.0 International License

Cardiorespiratory alterations in a newborn ovine model of systemic viral inflammation

Stéphanie Nault,¹ Sophie Tremblay,² Roqaya Imane,² Sally Al-Omar,¹ Charlene Nadeau,¹
Nathalie Samson,¹ Vincent Creuze,³ Guy Carrault,⁴ Patrick Pladys,⁴ and Jean-Paul Praud^{1*}

¹Neonatal Respiratory Research Unit, Departments of Pediatrics and Pharmacology-Physiology,
Université de Sherbrooke, QC, Canada

²Departments of Neurosciences and Pediatrics, CHU Sainte-Justine Research Center, Faculty of
Medicine, Université de Montréal, QC, Canada

³LIRMM, Univ Montpellier, CNRS, Montpellier, France

⁴Inserm, LTSI – UMR 1099, F-35000, Université Rennes 1, CHU Rennes, Rennes, France.

Author contributions: Each author has met the *Pediatric Research* authorship requirements. GC, JPP, NS, PP, RI, SAO, SN, ST, VC conceived and designed the research; CN and SN performed experiments; CN, GC, NS, PP, RI, SAO, SN, ST and VC analyzed data; SN, ST, VC, GC, PP and JPP interpreted results of experiments; SN, ST, RI and VC prepared figures; SN drafted manuscript; GC, JPP, NS, PP, RI, SN, and ST edited and revised manuscript. All authors approved the final version of manuscript.

Running title: Cardiorespiratory control and viral sepsis

Corresponding author:

* Jean-Paul Praud MD PhD (jean-paul.praud@usherbrooke.ca)

Departments of Pediatrics and Physiology

Université de Sherbrooke,

3001, 12e avenue Nord, Sherbrook, QC, Canada, J1H 5N4

Phone: (819) 346-1110, ext 75363

Statement of financial support: Patrick Pladys received funding from the European Union's Horizon 2020 research and innovation program under grant agreement no. 689260 (Digi-NewB project). Jean-Paul Praud received funding from the Canada Research Chair in Neonatal Respiratory Physiology. He is a member of the University of Sherbrooke Hospital Research Center, the Quebec Respiratory Research Network and the Quebec Perinatal Research Network. Sophie Tremblay received funding from the Scottish Rite Charitable Foundation of Canada and the Canadian Institutes of Health Research.

Disclosure statement: There is no disclosure

Category of study: Basic science

Consent statement: No patient consent was required

Impact:

- Provides unique observations on the cardiorespiratory consequences of injecting Poly I:C in a full-term newborn lamb to mimic a systemic inflammation secondary to a viral sepsis.
- Poly I:C injection led to a biphasic increase in rectal temperature and heart rate associated with an overall decrease in heart-rate variability, with no change in respiratory-rate variability.
- Brainstem inflammation was found in the areas of the cardiorespiratory control centers.

ABSTRACT

Respiratory viruses can be responsible for severe apneas and bradycardias in newborn infants. The link between systemic inflammation with viral sepsis and cardiorespiratory alterations remains poorly understood. We aimed to characterize these alterations by setting up a full-term newborn lamb model of systemic inflammation using polyinosinic:polycytidylic acid (Poly I:C). Two 6-hour polysomnographic recordings were carried out in eight lambs on two consecutive days, first after an IV saline injection, then after an IV injection of 300 µg/kg Poly I:C. Poly I:C injection decreased locomotor activity and increased NREM sleep. It also led to a biphasic increase in rectal temperature and heart rate. The latter was associated with an overall decrease in heart-rate variability, with no change in respiratory-rate variability. Lastly, brainstem inflammation was found in the areas of the cardiorespiratory control centers 6 hours after Poly I:C injection. In conclusion, the alterations in heart-rate variability induced by Poly I:C injection may be, at least partly, of central origin. Meanwhile, the absence of alterations in respiratory-rate variability is intriguing and noteworthy. Although further studies are obviously needed, this might be a way to differentiate bacterial from viral sepsis in the neonatal period.

INTRODUCTION

Late-onset sepsis (LOS)—a frequent complication in preterm infants in the neonatal intensive care unit—is often associated with severe cardiorespiratory events, which bear their own significant morbidity and mortality^{1,2,3}. Typically, neonatal sepsis is considered of bacterial origin until proven otherwise, but bacterial cultures frequently return negative⁴. Many viruses,—including coronavirus, enterovirus, human metapneumovirus, influenza, parainfluenza, respiratory syncytial virus and rhinovirus—have also been reported to cause LOS in preterm infants⁵⁻⁷. Recognition of these viral infections remains challenging due to the wide range of clinical manifestations, which often are similar to bacterial infections^{7,8}. Early recognition of the viral origin of LOS is of high clinical importance to prevent the adverse effects of indiscriminate antibacterial treatment in infants and reduce the length of hospital stay^{4,9}.

The early diagnosis of a viral infection is also important in full-term infants. Viruses such as rhinovirus, influenza virus, and respiratory syncytial virus can be responsible for severe apneas and bradycardias in the first weeks of life^{7,10,11}. These viruses have also been involved in sudden infant death syndrome¹²⁻¹⁵.

Polyinosinic:polycytidylic acid (Poly I:C) is a synthetic double-stranded RNA that, like viruses, binds to Toll-like receptor 3 (TLR3)^{16,17}. This consequently activates the NF- κ B pathway, a central mediator of pro-inflammatory gene induction and functions in immune cells¹⁸. Experimental studies have used Poly I:C to assess various aspects of viral sepsis in adult rats^{19,20}, mice²¹, rabbits²²⁻²⁴, guinea pigs²⁵, and rhesus monkeys²⁶. These studies have focused, however, on acute-phase reaction. To our knowledge, the cardiorespiratory alterations observed in response to Poly I:C injection have not been previously assessed, and no studies using Poly I:C to mimic viral sepsis have been performed in the neonatal period. The main goal of the present study was therefore to characterize the physiological consequences of the systemic inflammation induced by Poly-I:C injection in the full-term newborn lamb. We particularly focused on the cardiorespiratory alterations observed during the first six hours following this injection, in relation to the clinical need to find early markers of viral sepsis. Potential differences between these

alterations and those reported following lipopolysaccharide injection²⁷ will be discussed, aiming to identify features that could discriminate between bacterial and viral sepsis in the neonatal period. A second goal of this study was to assess whether inflammation was present in the areas of the cardiorespiratory control centers of the brainstem following Poly I:C injection in our neonatal ovine model.

MATERIAL AND METHODS

The protocol of the study was approved by the Ethics Committee for Animal Care and Experimentation of the Université de Sherbrooke; the experiment was performed in keeping with the recommendations of the Canadian Council on Animal Care. Sixteen full-term, male mixed-bred lambs, aged 2–4 days and weighing 3.3 ± 0.5 kg (range: 2.6–4.2 kg), were included in this crossover design study. More precisely, eight lambs were used for studying the systemic inflammation and cardiorespiratory alterations induced by Poly I:C injection, and eight control lambs were used to assess brainstem inflammation. In the first-ever study on the potential for Poly I:C injection to provide a model of early-life sepsis, we chose to include only male lambs. This is supported by literature data reporting that male sex is a well-known risk factor for SIDS²⁸ and might also be associated with late-onset sepsis in preterm infants²⁹.

Chronic instrumentation and recording equipment

As explained in a prior publication by our team²⁷, following intramuscular injections of ketoprofen 3 mg/kg, atropine sulfate 0.1 mg/kg and ketamine 5 mg/kg, a catheter was inserted into the left carotid artery under local anesthesia (2% lidocaine) for monitoring systemic arterial blood pressure and for measuring arterial blood gases. General anesthesia was not used in order to avoid its effects on heart-rate and respiratory-rate variability³⁰. Ampicillin (50 mg) and tobramycin (5 mg/kg) were injected intramuscularly once a day until the end of the experiments.

The following sensors were added on the recording days: (i) subcutaneous needle electrodes (MVAP Medical Supplies, Thousand Oaks, CA) to record electroencephalogram (EEG), electrooculogram (EOG) and electrocardiogram (ECG); (ii) respiratory inductance plethysmography bands on the chest and abdomen to record lung-volume variations (Ambulatory Monitoring, Ardsley, NY); (iii) a pulse oximeter reflectance sensor (LNOP YI, Masimo Radical, Irvine, CA) at the base of the tail to record oxygen hemoglobin saturation (SpO₂); and (iv) a rectal probe to record core body temperature.

Physiological signals were transmitted wirelessly using our custom-designed radiotelemetry system³¹ and recorded on a PC with AcqKnowledge software (version 4.1, Biopac Systems, Montreal, Canada).

Design of the study

The lambs were housed unrestrained in a Plexiglas chamber and were able to move and feed *ad libitum* from a custom-built lamb feeder³². As previously described³³, an infrared video camera above the Plexiglas chamber continuously monitored their locomotor activity.

Neonatal ovine model of systemic inflammation induced by Poly I:C injection

An intravenous injection of Poly I:C (InvivoGen, San Diego, CA, USA) was used to mimic a systemic viral inflammation. Poly I:C is a synthetic ligand of TLR3, which is involved in rhinovirus, influenza and respiratory syncytial virus infections¹¹.

Following a 24-hour recovery period after surgery, the nonsedated lambs underwent two 6-hour recordings on two consecutive mornings. On the first day, an intravenous bolus of 10 mL of normal saline solution (saline condition) was injected, whereas an intravenous bolus of 10 mL of Poly I:C (300 µg/kg) was administered on the second day (Poly I:C condition). Arterial blood gas measurement was performed at baseline, and repeated at 3 and 6 hours after injection (RapidLab 348, Siemens Healthcare Limited, Oakville, Canada). Following completion of the second-day recording, euthanasia was performed by an intravenous injection of 90 mg/kg of pentobarbital sodium.

Data analysis

Video analysis of locomotor activity. The total distance traveled and the percentage of time the animal was active throughout the recordings were calculated with custom-built software, as previously described²⁷.

States of alertness. Quiet and active wakefulness, as well as non-rapid eye movement (NREM) and rapid eye movement (REM) sleep were defined in keeping with standard electrophysiological and behavioral criteria³⁴.

Cardiac and respiratory function. Electrocardiogram, arterial blood pressure and respiratory movements were continuously recorded for 6 hours in both saline and Poly I:C conditions. The following variables were calculated every 15 minutes, as previously reported²⁷: (i) respiratory frequency (f_R) averaged on 60 seconds, and heart rate (HR) and mean arterial pressure averaged on 30 seconds; (ii) the number of apneas (defined as at least two missed breaths) and total apnea duration; (iii) the number of cardiac decelerations (defined as a decrease in HR greater than 30% lasting less than 5 seconds); and (iv) the number of bradycardias (defined as cardiac decelerations lasting at least 5 seconds).

Heart-rate and respiratory-rate variability. Heart-rate and respiratory-rate variability analysis were performed as previously described^{27,35}. The procedure is detailed in the section on “Heart-rate and respiratory-rate variability” of the Supplementary Material and will only be summarized here. Analyses were performed blindly with regard to the condition: saline or Poly I:C.

For heart-rate variability (HRV), following automatic extraction of all the 2-minute stationary periods from each 6-hour recording, QRS complexes were automatically detected. Thereafter, the quality of each RR (cardiac-cycle length) series obtained was checked visually and corrected when necessary. Time-domain analysis of HRV included the mean and standard deviation (SD) of RR duration and the square root of the mean squared differences of successive RR intervals (rMSSD). The complexity and regularity of the RR series were assessed by computing the sample entropy (SampEn). Frequency-domain analysis was performed through estimation of the power spectrum and integration of the low-frequency (LF, 0.02–0.25 Hz) and high-frequency (HF, 0.25–2 Hz) spectral bands³⁶, and computation of the LF/HF ratio. In addition, the following nonlinear analyses were performed: assessment of the short-term (SD1) and long-term (SD2) variability using the Poincaré plot; computation of the acceleration (AC) and deceleration

capacity (DC); and computation of the fractal scaling exponent α_1 of the detrended fluctuation analysis technique to test for the scale invariance. Lastly, HRV analyses based on the representations of the horizontal and vertical visibility networks³⁷⁻³⁹ were used to provide novel global insight into HRV. The resulting dimensionless network representations (see Supplementary Material, paragraph entitled “A simple introduction to horizontal and vertical visibility graphs” in reference 1 for a simplified, step-by-step explanation) are based on the organization of connectivity between the different durations of successive cardiac cycles. Alterations in network graphic representations can be visually recognized and quantified by computing several variables, including the mean degree, assortativity, and transitivity⁴⁰. For respiratory-rate variability, linear analyses in the time domain were performed on Ttot series and included mean and SD computation, while nonlinear analyses included Poincaré plots (SD1 and SD2) and sample entropy (SampEn). Lastly, cardiorespiratory interrelations were studied by computing the Pearson r^2 and the nonlinear h_2 correlation coefficients, the mean phase coherence $\gamma_{RR,RESP}$, and the amplitude of the respiratory-sinus arrhythmia³⁵.

Measurement of brainstem inflammation

The second objective of the study was to assess whether Poly I:C injection induces brainstem inflammation, especially in the areas where the cardiorespiratory control centers are located. To assess brainstem inflammation, Poly I:C lambs (n = 8) were randomly divided in two groups, one for real-time quantitative PCR studies (n = 4) and the other for histological studies (n = 4). The same operation was carried out for the eight control lambs. Analyses were performed blindly with regard to the group: control or Poly I:C. We searched for reactive microglia in the areas of the nucleus tractus solitarius and the rostral ventrolateral medulla, and if inflammatory mediators were increased in the medulla oblongata. Methods

used in this study have been described previously and are detailed in the Supplementary Data. Only a short summary is provided herein.

Analysis of microglial-cell activation. The resident microglial cells in the nervous system can be activated by Poly I:C⁴¹ and, in turn, produce various inflammatory mediators, such as IL-8 and TNF- α ⁴²⁻⁴⁴. Brainstems were dissected from the whole brains, and half of each brainstem was fixed in 10% formalin solution. Sagittal sections 16 μ m thick were performed serially from the medial to the lateral brainstem. They were incubated overnight with anti-Iba1 (microglia) and anti-GFAP (astrocytes) primary antibodies, then with fluorescent-dye conjugated secondary antibodies. Microglial cells of the rostral ventrolateral medulla and the nucleus tractus solitarius were imaged with a Leica TCS SP8 confocal microscope. A total of 12 images per lamb (four sections \times three images per section) were studied in Poly I:C lambs and compared to the same number of images in control lambs. The images were preprocessed with ImageJ to compute the number of microglial cells and assess their morphology. A quantitative 3D-morphological analysis of each image was then performed with 3DMorph automatic analysis software to provide the individual volume of microglial cells as well as their total territorial volume.

Real-time quantitative PCR. The medulla oblongata was kept in a TRIzol solution at -80°C , followed by total RNA extraction and verification of RNA integrity. Reverse transcription and quantitative PCR amplification were then performed in triplicate with the appropriate primers for the early-onset inflammatory and apoptosis mediators IL-6, IL-8, TNF- α , and caspase-3. The PCR probes and primers used are reported in Table 1 in the Supplementary Material.

Statistical analysis

Statistical analyses were performed under close guidance of the biostatistics department of our research center. All analyses were carried out on raw data for all dependent variables and expressed as median

(Q1, Q3). Since all quantitative variables—rectal temperature, locomotor activity, states of alertness, apnea number, total apnea duration, cardiac deceleration and bradycardia number, total cardiac deceleration duration, heart-rate and respiratory-rate variability, cardiorespiratory interrelations—did not follow a normal distribution (Shapiro-Wilk test), the Wilcoxon signed-rank test was used to assess the effect of Poly I:C injection for all comparisons (SPSS Statistics, version 25, Armonk, NY). A sensitivity power analysis based on a Wilcoxon signed-rank test concluded that the minimum detectable standardized difference—Cohen’s d_z , expressed in standard deviation units⁴⁵— was 1.2 with a significance level of 5%, a power of 80% and a sample size of 8 (G*Power software version 3.1.9.7, Heinrich Heine University, Germany).

In addition, to evaluate the association between independent variables (recording time points, temperature and Poly I:C injection) and each outcome variables (respiratory frequency, heart rate and mean arterial pressure), mixed models were used (SAS Institute Inc., version 9.3, Cary, NC). Since multiple measurements were made in each lamb, a random effect on intercept and a first-order autoregressive structure of the residuals were specified in the covariance structure of the mixed models (PROC MIXED in SAS). Linear, quadratic and cubic associations were studied for time and temperature, considering each day separately, and included in the multivariable models if significant. Differences were considered significant if $p < 0.05$.

RESULTS

Main objective of the study

Core body temperature

Contrarily to the saline condition, Poly I:C injection induced a biphasic increase in core body temperature in all lambs with a first peak at approximately 45 minutes ($\Delta T = 1^\circ\text{C}$; $p = 0.04$), followed by a second, longer, and more sustained increase peaking around 150 minutes ($\Delta T = 1.3^\circ\text{C}$; $p = 0.03$). Thereafter, core body temperature gradually decreased back to baseline level around 280 minutes post-Poly I:C injection (Figure 1).

Locomotor activity

Video analysis ($n = 7$ lambs) revealed that, compared to the saline condition, Poly I:C injection markedly decreased the total distance traveled [108.3 (82, 142.9) vs. 46.3 (43.1, 70.6) m, $p = 0.02$] (Figure 2A and Figure 2C) and the percentage of time the animal was active [0.9% (0.8, 1.3) vs. 1.8% (1.5, 2.9), $p = 0.03$] (Figure 2B) compared to the saline condition.

States of alertness

Poly I:C injection significantly increased the percentage of recording time spent in NREM sleep [18 (12, 21) vs. 25 (21, 28) %, $p = 0.01$] and significantly decreased the percentage of time spent in active wakefulness [21 (13, 25) vs. 11 (9, 12) %, $p = 0.01$] compared to the saline condition. No statistical differences were noted for quiet wakefulness [53 (49, 58) vs. 60 (48, 61) %, $p = 0.4$] and REM sleep [6 (4, 7) vs. 5 (3, 7) %, $p = 0.5$] between the Poly I:C and saline conditions.

Arterial blood gases

Arterial blood gases ($n = 7$) revealed that PaO_2 at the 6-hour time point was significantly increased [71 (58, 103) vs. 91 (87, 100) mmHg, $p = 0.04$] after Poly I:C injection compared to the saline condition. No statistical differences were observed for PaCO_2 , pH, or HCO_3^- between the conditions (Table 1).

Effect of Poly I:C injection on cardiorespiratory control system

Respiratory activity. Overall, when averaged over the 6-hour recording, no significant change was observed in f_R [55 (51, 56) vs. 52 (49, 58) $\cdot \text{min}^{-1}$, $p = 0.9$] between the saline and Poly I:C conditions respectively (Figure 3A). The biphasic time course of f_R variations followed that of temperature, however, so that, for each increase of 1° in temperature, the f_R increased by 7.4 breaths per minute ($p < 0.0001$) (Figure 3A). In addition, the number [21 (7, 37) vs. 8 (3, 31), $p = 0.08$] and the total duration of apneas [86 (27, 203) vs. 38 (16, 133) s, $p = 0.1$] were not different between the saline and Poly I:C, respectively (Figure 4A). Furthermore, no change in respiratory-rate variability was observed when measured in the 2-minute stationary periods after Poly I:C injection (Table 2).

Cardiac activity. Overall, conversely to f_R , Poly I:C injection significantly increased the mean HR compared to the saline condition [183 (180, 195) vs. 254 (244, 268) $\cdot \text{min}^{-1}$, $p = 0.001$] (Figure 3B). Similarly to f_R , the biphasic time course of HR variations followed that of temperature, so that, for each increase of a degree in temperature, the HR increased by 17 beats per minute ($p < 0.0001$). Moreover, the number [81 (23, 127) vs. 53 (25, 72) $p = 0.3$] and the total duration of cardiac decelerations [66 (22, 96) vs. 32 (17, 61) s, $p = 0.2$] was not different between the saline and Poly I:C conditions, respectively (Figure 4B). No bradycardia longer than 5 seconds was observed in either condition. Of note, however, when observed in the 2-minute stationary periods only, the increase in HR expressed by the decrease in mean RR interval exceeded 2 standard deviations of the HR observed in the saline condition after 58 minutes and reached a first maximum at 116 minutes, which corresponded to an amplitude of change of 4 standard deviations.

The overall significant decrease in mean RR observed in all lambs was associated with a decrease in HRV; this included a decrease in SD (total heart rate variability), and in SD1 and HF (parasympathetic activity), with marginal changes in LF/HF and SampEn (Table 2). Notably, results computed from the network representations of the horizontal and vertical visibility analyses showed a highly significant

decrease in vertical and horizontal assortativity and horizontal transitivity, as well as an increase in vertical mean degree (Table 2).

Mean systemic arterial blood pressure. Overall, no significant difference was observed between the saline and Poly I:C conditions [69 (67, 71) vs. 65 (64, 66) mmHg respectively, $p = 0.4$]. Moreover, contrarily to HR and f_R , there was no significant relationship between mean arterial pressure and temperature (Figure 3C).

Cardiorespiratory interrelations. A decrease in the magnitude of the respiratory-sinus arrhythmia was observed, indicating a significant decrease in cardiorespiratory interactions (Table 2).

Increased brainstem inflammation

Figures 6A–G illustrate the results on reactive microglial cells in the rostral ventrolateral medulla (RVLM) and the nucleus tractus solitarius (NTS) for the control vs. Poly I:C lambs. The quantitative 3DMorph analysis of microglia cells showed a significantly larger cell-body volume in both the RVLM [651 (586) [median(interquartile range)] vs. 759 (1700) μm^3 , $p = 0.0009$] and the NTS [621 (624) vs. 675 (929) μm^3 , $p = 0.02$] in the Poly I:C lambs (Figure 6J). These brainstem areas also had a larger territory occupied by microglial cells in the Poly I:C lambs, the statistical significance being reached in the RVLM areas only (RVLM: 4785 (5883) vs. 5913 (12530) μm^3 , $p = 0.001$); NTS: 5716 (7914) vs. 6005 (12116) μm^3 , $p = 0.09$; Figure 6K). Meanwhile, qualitative assessment of astrogliosis did not suggest any differences between control and Poly I:C lambs in the same brainstem areas.

In addition, an increase in mRNA expression of IL-6, IL-8, TNF- α , and caspase-3 was observed in the medulla oblongata 6 hours after Poly I:C systemic injection (Figure 6L).

DISCUSSION

The current study provides new observations on the physiological consequences of injecting Poly I:C to mimic a systemic inflammation related to viral sepsis in a full-term newborn ovine model. The general effects of Poly I:C within the 6 hours following injection included a biphasic increase in core body temperature and a decrease in locomotor activity and active wakefulness, as well as an increase in NREM sleep. Moreover, Poly I:C injection led to variations in both HR and f_R following a biphasic pattern paralleling temperature variations. In addition, Poly I:C injection was responsible for an overall decrease in HRV (mainly in parasympathetic activity) and a loss of entropy, indicating a decrease in the cardiac regulatory capacity. No significant alteration of RRV was found. Lastly, the presence of reactive microglia was observed 6 hours after Poly I:C injection in the ventrolateral and dorsal areas of the medulla oblongata containing the cardiorespiratory control centers, together with an increase in IL-6, IL-8, TNF- α , and caspase-3 mRNA expression in the medulla oblongata.

Our neonatal ovine model of Poly I:C viral sepsis

Most viruses produce double-stranded RNA at some point during their replication⁴⁶. Compared to live viruses, the use of Poly I:C—a synthetic viral double-stranded RNA analog—has the advantages of safety, reproducibility, and control over dose and time of administration²⁰. Poly I:C induces TLR3 stimulation, which is especially involved in rhinovirus, coronavirus, influenza, and respiratory syncytial virus infection^{10,11,47}. The latter frequently presents as severe cardiorespiratory events in the first weeks of life in both the full-term and preterm infant and has been suggested as an important triggering factor of sudden infant death syndrome^{13,15}.

An extensive review of the literature revealed that only two studies used Poly I:C in sheep^{48,49}. The first study focused on the developmental changes in TLRs in a fetal sheep lung⁴⁸, while the second study used Poly I:C to define the innate immune response caused by bluetongue virus in adult sheep and goats⁴⁹. A

variety of other animal species were used to study acute-phase reaction, fever, sickness behaviors, and pyrogenic properties of central or systemic administration of Poly I:C. As already alluded to, none of these studies were performed in the neonatal period. In addition, none examined the effects of Poly I:C on cardiorespiratory control alterations. The present study therefore provides unique observations—especially in terms of cardiorespiratory alterations—of systemic inflammation consequent to TLR3 activation in a newborn animal model.

Potential confounding effect of the medications used on our study results

Surgical instrumentation was necessary for recording cardiorespiratory variables for several hours. In order to avoid the significant effects of general anesthesia on cardiorespiratory function, we purposely used conscious sedation with ketamine instead. Although we do not find specific literature on the subject in sheep, a study in humans showed that the effects of a ketamine infusion on heart rate variability was back to normal after 24 hours⁵⁰. This suggests that ketamine did not have any effect on our results. In any event, if ketamine effects had persisted, we would have expected their inhibitory action on parasympathetic activity to predominate 24 hours after ketamine injection, i.e., the saline condition. On the contrary, this parasympathetic activity was lower on the second experimental day (i.e., Poly I:C injection compared to the saline condition).

Given that the half-life of atropine is 1.6 hours in sheep⁵¹, we do not believe that atropine could have had any significant effects on our results. Again, the effect of atropine—a decrease in parasympathetic activity—would have predominated on the first experimental day, i.e., the saline condition. On the contrary, we found that the sympathetic activity was lower on the second experimental day (i.e., Poly I:C compared to the saline condition).

As for ketoprofen, given its short half-life (< 1 h) in the sheep⁵², we do not believe the low blood level remaining 48 hours after its injection would significantly blunt the inflammatory effect of Poly I:C. Accordingly, a robust and strong effect was observed in all the lambs following Poly I:C injection.

Effect of Poly I:C administration on core body temperature

Poly I:C robustly induced a biphasic increase in core body temperature at 45 and 150 minutes after injection in all lambs. This biphasic pattern is in agreement with past results in rabbits (bolus 50 µg/kg Poly I:C)²³. In contrast, monophasic fever was observed in rats^{19,20}, mice²¹, rabbits^{22,24}, and guinea pigs²⁵. Differences between studies might be due to the animal species, the route of administration, and/or the dose of Poly I:C used. The doses of Poly I:C used in the literature are variable—from 0.25 µg/kg to 25 mg/kg¹⁹⁻²⁶ and unknown in the newborn lamb. We selected a bolus of 300 µg/kg in our pilot studies as the lowest dose of Poly I:C which induced fever, one of the most common symptoms seen in septic children⁴. One previous study in rats suggested that fever following Poly I:C injection would result from the pyrogenic activity of inflammatory mediators (IL-1, IL-6, IFNs, and TNF-α)^{4,22,53}, which increase the synthesis of prostaglandin E₂. The latter, in turn, raises the set point of the thermoregulatory center in the hypothalamus^{4,53}.

Effect of Poly I:C administration on locomotor activity and sleep states

While lipopolysaccharide injection induced fever, and decreased locomotor activity and increased sleep in lambs^{27,55,56}, the effects of Poly I:C on sickness behavior is unknown in newborn animals. In the current study, Poly I:C injection decreased lamb locomotor activity and increased NREM sleep at the expense of active wakefulness. The mechanisms by which viruses might decrease activity and induce sleep are not well understood. Double-stranded RNA produced during viral replication might cause excessive sleep by direct toxic effects or via the production of interferon (INF-α) and pro-inflammatory cytokines (e.g., IL-1, TNF), which have somnogenic properties^{22,53,57}. This increase in NREM sleep in lambs is in agreement with results on Poly I:C in adult rabbits, which showed an increase in slow-wave sleep duration but an inhibition of REM sleep^{22,57}.

Effect of Poly I:C administration on cardiorespiratory control

The main focus of the current study was to investigate the effects of Poly I:C injection on neonatal cardiorespiratory control. To our knowledge, our research team is the first to study cardiorespiratory activity thoroughly following Poly I:C-injection.

The increase in HR we observed in all lambs is reminiscent of the tachycardia usually accompanying viral sepsis in children⁴. It can again be explained by Poly I:C-induced synthesis of pro-inflammatory cytokines (e.g., IL-6, IL-1 β , TNF- α)⁵⁸, which have an excitatory effect on the sympathetic branch of the autonomic nervous system. The increase in HR was associated with a decrease in HRV, which predominates on the short-term respiratory-related components, as measured by SD1, HF, and the magnitude of the respiratory sinus arrhythmia. In addition, it is noteworthy that results from the horizontal and vertical visibility analyses show significant changes in many indices (mean degree, assortativity, and transitivity) computed from network representations, suggesting the potential clinical importance of visibility analysis of HRV in diagnosing and managing viral sepsis in newborns. Physiologically, these observations overall likely reflect an alteration in the temporal structural organization of HR control, together with an increase in sympathetic activity and/or a decrease in vagal activity. These results are in agreement and extend past observations of decreased HRV during viral infection, including respiratory syncytial virus infection in young infants⁵⁹, enterovirus⁶⁰, and dengue⁶¹ infection in children, as well as SARS-CoV-2 infection in adults⁶².

Consequences of Poly I:C- vs. LPS-injection on the cardiorespiratory control system

The question remains whether the early alterations of cardiorespiratory control, which can be observed at the bedside, might help differentiate viral from bacterial infection in the newborn. A few differences between our observations following Poly I:C vs. LPS injection²⁷ are worthy of mention. While we found a biphasic increase in HR after either Poly I:C or LPS injection, the fact that the increase in HR was delayed and varied out of phase with body temperature for 6 hours after LPS²⁷ but not Poly I:C, is notable but remains unexplained. In addition, although a similar decrease in many HRV indices was observed

after either LPS or Poly I:C injection, it is also noteworthy that f_R and RRV were clearly altered following LPS (see Table 2 in 27), but unchanged following Poly I:C injection. Whether this notable difference might help differentiate viral from bacterial infection in the neonatal period remains to be confirmed. Overall, our results further support that HRV analyses are relevant to early diagnosis of neonatal sepsis; these include the visibility graph analysis of HRV^{27,63}. Our results also suggest, however, that HRV analyses might be insufficient to discriminate between bacterial and viral sepsis. Studying both RRV and HRV within a multivariate approach might improve the early diagnosis of bacterial sepsis⁶⁴. This remains to be validated in clinical contexts.

Brainstem inflammation

The increased mRNA expression of IL-6, IL-8, TNF- α , and caspase-3 in the medulla oblongata shows that Poly I:C induced inflammation in the brainstem. The significant wider territory and cell volume occupied by microglial cells—i.e., microglial activation—following Poly I:C injection confirm the presence of inflammation in the areas containing cardiorespiratory centers in newborn lambs. To our knowledge, this is the first evidence of microgliosis—together with increased pro-inflammatory cytokine profiles—induced in the brainstem by postnatal Poly I:C injection. This inflammation likely contributes to the acute alterations in the control of cardiac activity that we report herein. Of note, the interindividual variability in mRNA expression might be due to the variable delay between Poly I:C injection and the inflammatory response in the brain, similarly to our recent observations in newborn lambs following LPS-induced systemic inflammation²⁷. Beyond this local brainstem inflammation, prenatal exposure to viral infection is known to disrupt the normal expression of immune molecules by microglia, and to increase the risk for neurodevelopmental disorders including schizophrenia and autism spectrum disorder⁶⁵. Similarly, a single postnatal injection of Poly I:C was reported to have long-term negative effects on learning and memory through neuroinflammation⁶⁶. Developing clinical tools to distinguish

viral from bacterial infection at an early stage may help recognize neonates at risk for long-term neurological morbidities after viral exposure and promote better follow-up.

Study limitations

The main objective of the current study was to characterize the cardiorespiratory alterations observed during 6 hours after Poly I:C injection in full-term newborn lambs in an attempt to shed some light on the early cardiorespiratory consequences of neonatal viral sepsis. Our neonatal model has limitations as a model of systemic inflammation related to viral sepsis. Indeed, Poly I:C did not induce bradycardias or apneas—common clinical findings—which can reveal systemic infections in infants during the first weeks of life, especially in preterm infants with LOS⁵⁻⁷. While this is not surprising, since apneas-bradycardias associated with sepsis are less common in full-term than in preterm newborns—due to the general neural immaturity encompassing cardiorespiratory control⁶⁷—this constitutes a limitation of this study. These results are, however, important for viral sepsis in the very first postnatal weeks in full-term infants, as well as for paving the way for further studies in a preterm lamb model, in which the effect of prematurity will be readily inferred^{34,68,69}.

A second limitation is related to the use of Poly I:C injection, which cannot be considered as exactly mimicking a real viral sepsis. In addition, we do not know whether higher doses of Poly I:C or different routes of Poly I:C administration—such as the intranasal route—might differently alter cardiorespiratory activity, especially respiratory control.

Third, the choice to include male lambs only made it possible to test our hypothesis that Poly I:C can mimic some aspects of early-life sepsis, while reducing the number of lambs to a minimum for ethical reasons. This choice, however, is a limitation of our study, because the results could be different in female lambs, in agreement, for instance, with the well-known impact of sex on respiratory control⁷⁰. The impact

of sex on the effects of Poly I:C on cardiorespiratory control in newborn lambs will therefore have to be tested in future studies.

Fourth, the significant results obtained from both RT-PCR and analysis of microglial cell activation support the presence of brainstem inflammation in areas containing cardiorespiratory control centers 6 hours after Poly I:C injection. These results, however, were obtained in only a few lambs and will have to be confirmed in a greater number of lambs in future studies. These studies will also have to delineate the centers concerned by inflammation, such as, for instance, the pre-Bötzinger complex or the nucleus ambiguus, to provide further understanding of the effects of Poly I:C on cardiorespiratory control.

CONCLUSION

Viral infections are frequently unrecognized in newborn infants due to several challenges, including a wide range of clinical manifestations, which can be similar to bacterial infections⁷.

Results of our study using intravenous injection of Poly I:C in newborn lambs suggest that the early alterations in respiratory control, especially respiratory-rate variability, observed after bacterial infection might be less important or missing in the early phase of viral sepsis in the neonatal period. Similar studies in preterm lambs are needed to reveal the consequences of prematurity on the cardiorespiratory control alterations induced by LPS vs. Poly I:C injection, and to determine whether the alterations in respiratory control can still differentiate the two conditions.

REFERENCES

1. Mayr, F.B., Yende, S., Angus, D.C. Epidemiology of severe sepsis. *Virulence* **5**, 4–11 (2014).
2. Singer, M., et al. Third international consensus definitions for sepsis and septic shock (Sepsis-3). *JAMA* **315**, 801–810 (2016).
3. Shane, A.L., Sánchez, P.J., Stoll, B.J. Neonatal sepsis. *Lancet* **390**, 1770–1780 (2017).
4. Gupta N., Richter R., Robert S., Kong M. Viral sepsis in children. *Front. Pediatr.* **252**, 6 (2018).
5. Bennett, et al. Unrecognized viral respiratory tract infections in premature infants during their birth hospitalization: a prospective surveillance study in two neonatal intensive care units. *J. Pediatr.* **161**, 814–818 (2012).
6. Santos R.P., Tristram, D. A practical guide to the diagnosis, treatment, and prevention of neonatal infections. *Pediatr. Clin. North Am.* **62**, 491–508 (2015).
7. Cerone, J.B., et al. Incidence of respiratory viral infection in infants with respiratory syndroms evaluated for late-onset sepsis. *J. Perinatol.* **37**, 922–926 (2017).
8. Gagneur, A., et al. Outbreaks of human coronavirus in a pediatric and neonatal intensive care unit. *Eur. J. Pediatr.* **167**, 1427–1434 (2008).
9. Lin, G.L., McGinley, J.P., Drysdale, S.B., Pollard, A.J. Epidemiology and immune pathogenesis of viral sepsis. *Front. Immunol.* **9**, 2147 (2018).
10. Schroeder, A.R., et al. Apnea in children hospitalized with bronchiolitis. *Pediatrics* **132**, e1194–1201 (2013).
11. Rudd, B.D., Burstein, E., Duckett, C.S., Li, X., Lukacs, N.W. Differential role for TLR3 in respiratory syncytial virus-induced chemokine expression. *J. Virol.* **79**, 3350–3357 (2005).

12. Raza, M.W., Blackwell, C.C. Sudden infant death syndrome, virus infections and cytokines. *FEMS Immunol. Med. Microbiol.* **25**, 85–96 (1999).
13. Blood-Siegfried, J. The role of infection and inflammation in sudden infant death syndrome. *Immunopharmacol. Immunotoxicol.* **31**, 516–523 (2009).
14. Moscovis, et al. Virus infections and sudden death in infancy: The role of interferon- γ . *Front. Immunol.* **6**, 107 (2015).
15. Carlin, R.F., Moon, R.Y. Risk factors, protective factors, and current recommendations to reduce sudden infant death syndrome: A review. *JAMA Pediatr.* **171**, 175–180 (2017).
16. Jensen, S., Thomsen, A.R. Sensing of RNA viruses: a review of innate immune receptors involved in recognizing RNA virus invasion. *J. Virol.* **86**, 2900–2010 (2012).
17. Kawasaki, T., Kawai, T. Toll-like receptor signaling pathways. *Front. Immunol.* **5**, 461 (2014).
18. Liu, T., Zhang, L., Joo, D., Sun, S.C. NF- κ B signaling in inflammation. *Signal Transduct. Target Ther.* **2**, 17023 (2017).
19. Chuang, J., Lin, M.T., Chan, S.A., Won, S.J. Febrile effects of polyriboinosinic acid: polyribocytidylic acid and interferon: relationship to somatostatin in rat hypothalamus. *Pflugers Arch.* **415**, 606–610 (1990).
20. Fortier, M.E., et al. The viral mimic, polyinosinic:polycytidylic acid, induces fever in rats via an interleukin-1 dependent mechanism. *Am. J. Physiol. Regul. Integr. Comp. Physiol.* **287**, R759–R766 (2004).
21. Hiramoto, R.N., Ghanta, V.K., Rogers, C.F., Hiramoto, N.S. Conditioning the elevation of body temperature, a host defensive reflex response. *Life Sci.* **49**, 93–99 (1991).

22. Krueger, J.M., Majde, J.A., Blatteis, C.M., Endsley, J., Ahokas, R.A., et al. Polyriboinosinic:polyribocytidylic acid enhances rabbit slow-wave sleep. *Am. J. Physiol.* **225**, R748–R755 (1988).
23. Soszynski, D., Kozak, W., Szewczenko, M. Course of fever response to repeated administration of sublethal doses of lipopolysaccharides, polyinosinic: polycytidylic acid and muramyl dipeptide to rabbits. *Experientia* **47**, 43–47 (1991).
24. Kimura, M., Toth, L.A., Agostini, H., Cady, A.B., Majde, J.A., et al. Comparison of acute phase responses induced in rabbits by lipopolysaccharide and double-stranded RNA. *Am. J. Physiol.* **267**, R1596–605 (1994).
25. Cooper, K.E., Blähser, S., Malkinson, T.J., Merker, G., Zeisberger, E. Changes in body temperature and vasopressin content of brain neurons, in pregnant and non-pregnant guinea pigs, during fevers produced by Poly I:Poly C. *Pflugers Arch.* **412**, 292–296 (1988).
26. Bauman, M.D., et al. Activation of the maternal immune system during pregnancy alters behavioral development of rhesus monkey offspring. *Biol. Psychiatry* **75**, 332–341 (2014).
27. Nault, S., et al. Cardiorespiratory alterations in a newborn ovine model of systemic inflammation induced by lipopolysaccharide injection. *Front. Physiol.* **11**, 585 (2020).
28. Moscovis, S.M., Hall, S.T., Burns, C.J., Scott, R.J., Blackwell, C.C. The male excess in sudden infant deaths. *Innate Immun.* **20**, 24-29 (2014).
29. Battarbee, A.N., Glover, A.V., Vladutiu, C.J., Gyamfi-Bannerman, C., Aliaga, S., et al. Sex-specific differences in late preterm neonatal outcomes. *Am J Perinatol.* **36**, 1223-1228 (2019).
30. Venet, T., Pichot, V., Charier, D., Scalabre, A., Patural, H. Autonomic cardiac regulation after general anesthesia in children. *Paediatr. Anaesth.* **28**, 881–887 (2018).

31. Samson, N., Dumont, S., Specq, M.L., Praud, J.P. Radio telemetry devices to monitor breathing in non-sedated animals. *Respir. Physiol. Neurobiol.* **179**, 111–118 (2011).
32. Duvareille, C., et al. Validation of a new automatic smoking machine to study the effects of cigarette smoke in newborn lambs. *Lab. Anim.* **44**, 290–297 (2010).
33. Porée, F., et al. Non-invasive devices and methods for large animal monitoring using automated video processing. *IRBM* **35**, 173–181 (2014).
34. Renolleau, S., Letourneau, P., Niyonsenga, T., Praud, J.P. Thyroarytenoid muscle electrical activity during spontaneous apneas in preterm lambs. *Am. J. Respir. Crit. Care Med.* **159**, 1396–1404 (1999).
35. Al-Omar, S., et al. Assessment of tobacco smoke effects on neonatal cardiorespiratory control using a semi-automated processing approach. *Med. Biol. Eng. Comput.* **56**, 2025–2037 (2018).
36. Beuchée, A., et al. Prolonged dynamic changes in autonomic heart rate modulation induced by acid laryngeal stimulation in nonsedated lambs. *Neonatology* **91**, 83–91 (2007).
37. Lacasa, L., Luque, B., Ballesteros, F., Luque, J., Carlos Nuño, J. From time series to complex networks: The visibility graph. *Proc. Natl. Acad. Sci. USA.* **105**, 4972–4975 (2008).
38. Madl, T. Network analysis of heart beat intervals using horizontal visibility graphs. 2016 Computing in Cardiology Conference. 733–736 (2016).
39. Nguyen Phuc Thu, T., et al. Improving methodology in heart rate variability analysis for the premature infants: Impact of the time length. *PloS one* **14**, e0220692 (2019).
40. Luque, B., Lacasa, L., Ballesteros, F., Luque, J. Horizontal visibility graphs: Exact results for random time series. *Physical Review.* **80**, 046103 (2009).
41. Town, T., Jeng, D., Alexopoulou, L., Tan, J., Flavell, R.A. Microglia recognize double-stranded RNA via TLR3. *J. Immunol.* **176**, 3804–3812 (2006).

42. Ehrlich, L.C., et al. Cytokine regulation of human microglial cell IL-8 production. *J. Immunol.* **160**, 1944–1948 (1998).
43. Hanisch, U.K. Microglia as a source and target of cytokines. *Glia* **40**, 140–155 (2002).
44. Welser-Alves, J. V., Milner, R. Microglia are the major source of TNF- α and TGF- β 1 in postnatal glial cultures; regulation by cytokines, lipopolysaccharide, and vitronectin. *Neurochem. Int.* **63**, 47–53 (2013).
45. Cohen J. *Statistics power analysis for the behavioral sciences*. Chapter 2, the t test for means. Lawrence Erlbaum Associates, New York, Second edition, 1988, p. 48.
46. Jacobs, B.L., Langland, J.O. When two strands are better than one: the mediators and modulators of the cellular responses to double-stranded RNA. *Virology* **219**, 339–349 (1996).
47. Loron, G., et al. COVID-19 Associated With Life-Threatening Apnea in an Infant Born Preterm: A Case Report. *Front. Pediatr.* **8**, 568 (2020).
48. Hillman, N.H., et al. Toll-like receptors and agonist responses in the developing fetal sheep lung. *Pediatr. Res.* **63**, 388–393 (2008).
49. Dhanasekaran, S., et al. Comparative analysis of innate immune response following in vitro stimulation of sheep and goat peripheral blood mononuclear cells with bluetongue virus – serotype 23. *Vet. Res. Commun.* **37**, 319–327 (2013).
50. Olbrich, S., Meyer, T., Seifritz, E., Palenicek, T., Brunowsky, M. Ketamine treatment in major depressions: predictive power of heart rate. *Biol. Psychiatry.* **83**, S55 (2018).
51. Haskell, S.R., Payne, M., Webb, A., Riviere, J., Craigmill, A.L. Antidotes in food animal practice. *J. Am. Vet. Med. Assoc.* **226**, 884–887 (2005).
52. Landoni, M.F., Comas, W., Mucci, N., Anglarilli, G., Bidal, D., et al. Enantiospecific pharmacokinetics and pharmacodynamics of ketoprofen in sheep. *J. Vet. Pharmacol. Ther.* **22**, 349–359 (1999).

53. Harris, R.L., et al. Manifestations of sepsis. *Arch. Intern. Med.* **147**, 1895–1906 (1987).
54. Krueger, J.M., Majde, J.A. Microbial products and cytokines in sleep and fever regulation. *Crit. Rev. Immunol.* **37**, 291–315 (2017).
55. Billiards, S. S., Walker, D. W., Canny, B. J., and Hirst, J. J. Endotoxin increases sleep and brain allopregnanolone concentrations in newborn lambs. *Pediatr. Res.* **52**, 892–899 (2002).
56. McClure, L., et al. Effects of age and pregnancy on the circulatory activin response of sheep to acute inflammatory challenge by lipopolysaccharide. *J. Endocrinol.* **185**, 139–149 (2005).
57. Shoham, S., Davenne, D., Cady, A.B., Dinarello, C.A., Krueger, J.M. Recombinant tumor necrosis factor and interleukin 1 enhance slow-wave sleep. *Am. J. Physiol.* **253**, R142–R149 (1987).
58. Badke, C. M., Marsillio, L. E., Weese-Mayer, D. E., Sanchez-Pinto, L. N. Autonomic nervous system dysfunction in pediatric sepsis. *Front. Pediatr.* **6**, 280 (2018).
59. Stock, C., Teyssier, G., Pichot, V., Goffaux ,P., Barthelemy, J.C. Autonomic dysfunction with early respiratory syncytial virus-related infection. *Auton. Neurosci.* **156**, 90–95 (2010).
60. Lin, M.T., et al. Heart rate variability monitoring in the detection of central nervous system complications in children with enterovirus infection. *J. Crit. Care* **21**, 280–286 (2006).
61. Carter, R. 3rd, Hinojosa-Laborde, C., Convertino, V.A. Heart rate variability in patients being treated for dengue viral infection: new insights from mathematical correction of heart rate. *Front. Physiol.* **5**, 46 (2014).
62. Mageed, N.A., Abd El Baser, I.I. Predictive and Prognostic Value of Heart Rate Variability Analysis in Early Bedside Diagnosis and Management of COVID-19 Patients. *Anaest. Surg. Open Access J.* **1**, 5 (2020).

63. Leon, C., Carrault, G., Pladys, P., Beuchee, A. Early detection of late onset sepsis in premature infants using visibility graph analysis of heart rate variability. *IEEE J. Biomed. Health Inform.* **25**, 1006–1017 (2021).
64. Joshi, R., et al. Predicting neonatal sepsis using features of heart rate variability, respiratory characteristics, and ECG-derived estimates of infant motion. *IEEE J. Biomed. Health Inform* **24**, 681–692 (2020).
65. Haddad, F.L., Patel, S.V., Schmid S. Maternal immune activation by Poly I:C as a preclinical model for neurodevelopmental disorders: A focus on autism and schizophrenia. *Neurosci. Biobehav. Rev.* **113**, 546–567 (2020).
66. Baghel, M.S., Singh, B., Dhuriya, Y.K., Shukla, R.K., Patro, N., Khanna, V.K., Patro, I.K., Thakur, M.K. Postnatal exposure to poly (I:C) impairs learning and memory through changes in synaptic plasticity gene expression in developing rat brain. *Neurobiol. Learn. Mem.* **155**, 379-389 (2018).
67. Di Fiore, J.M., Poets, C.F., Gauda, E., Martin, R.J., MacFarlane P. Cardiorespiratory events in preterm infants: etiology and monitoring technologies. *J. Perinatol.* **36**, 165–171 (2016).
68. St-Hilaire, M., et al. Postnatal maturation of laryngeal chemoreflexes in the preterm lamb. *J. Appl. Physiol.* **102**, 1429–1438 (2007).
69. Nault, S., Samson, N., Nadeau, C., Djeddi, D., Praud, J.P. Reflex cardiorespiratory events from esophageal origin are heightened by preterm birth. *J. Appl. Physiol.* **123**, 489–497 (2017).
70. Rousseau, J.P., Tenorio-Lopes, L., Baldy, C., Janes, T.A., Fournier, S., et al. On the origins of sex-based differences in respiratory disorders: Lessons and hypotheses from stress neuroendocrinology in developing rats. *Respir Physiol Neurobiol.* **245**, 105-121 (2017).

ACKNOWLEDGMENTS

The authors wish to acknowledge the help of Marie-Pierre Garant, Biostatistics Division, Research Center of the Centre hospitalier universitaire de Sherbrooke (CRCHUS).

FIGURE LEGENDS

Figure 1. Changes in core body temperature in relation to time after intravenous injection of Poly I:C. Poly I:C induced a biphasic increase in rectal temperature in newborn lambs. ▲: peaks of temperature. Results are illustrated as mean \pm SD, $*p < 0.05$ vs. saline condition.

Figure 2. Video analysis of locomotor activity. The total distance traveled (A) (box-and-whisker plot) and the percentage of time the animal was active (B) were significantly decreased following Poly I:C injection vs. saline condition during the 6-hour recordings. (C) gives an example of trajectory plot in one lamb in saline and Poly I:C conditions.

Figure 3. Effects of Poly I:C injection on heart rate, respiratory frequency, and mean systemic arterial pressure. (A) Although no significant changes were observed for f_R between the Poly I:C and saline conditions, a significant relationship was found between f_R and temperature for the Poly I:C condition. (B) Poly I:C significantly increased heart rate compared to the saline condition, and a significant relationship was found between heart rate and temperature for the Poly I:C condition. (C) No differences were observed for MAP between the conditions. Left panel: saline condition; right panel: Poly I:C condition. f_R : respiratory frequency; T: temperature; HR: heart rate; MAP: mean systemic arterial pressure. Results are illustrated as mean \pm SD.

Figure 4. Effects of Poly I:C injection on apneas and cardiac decelerations. (A) Poly I:C injection did not change the number or the total duration of apneas. (B) Poly I:C injection did not change the number and the total duration of cardiac decelerations. Results are illustrated as box-and-whisker plots. No.: number. $*p < 0.05$ vs. saline condition.

Figure 5. Network representation of heart-rate variability analysis by graph visibility in one lamb in saline condition (A) and following Poly I:C injection (B).

(A) Evolution of an RR time series (left) and the corresponding dimensionless network representation of the vertical visibility graph analysis computed with a horizon of 30 points (right). Some noteworthy nodes are annotated in this saline condition. For example, nodes 79 and 161 (in black and magenta respectively), which are minima of the RR time series, have very few connections with the other nodes. Other nodes on the outer side are also minima. In contrast, nodes 24, 118, and 185 (in green, red, and light blue, respectively) are examples of maxima of the RR time series. The links (edges) in the same color show the multiple connections they have with the nearest neighbors in the network representation. These maxima-related nodes are separated by subnetworks of highly connected nodes (in blue), whose size is related to the horizon distance. Note the overall high density of the links between nodes, which reflects the high cardiac variability in saline condition.

(B) A similar illustration following Poly-IC injection in the same lamb. Similar to Figure 5A, nodes 84 and 157 (examples of minima of the RR time series) have very few connections with the other nodes. Contrary to Figure 5A (representing the saline condition), nodes 7, 115, and 184 (examples of maxima of the time series) are much less distinct nodes of the network. In addition, the subnetworks between these maxima-related nodes are less identifiable due to having fewer connections than the saline condition. Such decreased connectivity attests to the low heart-rate variability, indicating an abnormal and inadequate adaptation of the autonomic nervous system.

Of note, the orientation of the network representations has no particular meaning; it was only chosen to facilitate network interpretation.

Figure 6. Measurement of brainstem inflammation and microglial-cell morphological changes following systemic Poly I:C injection.

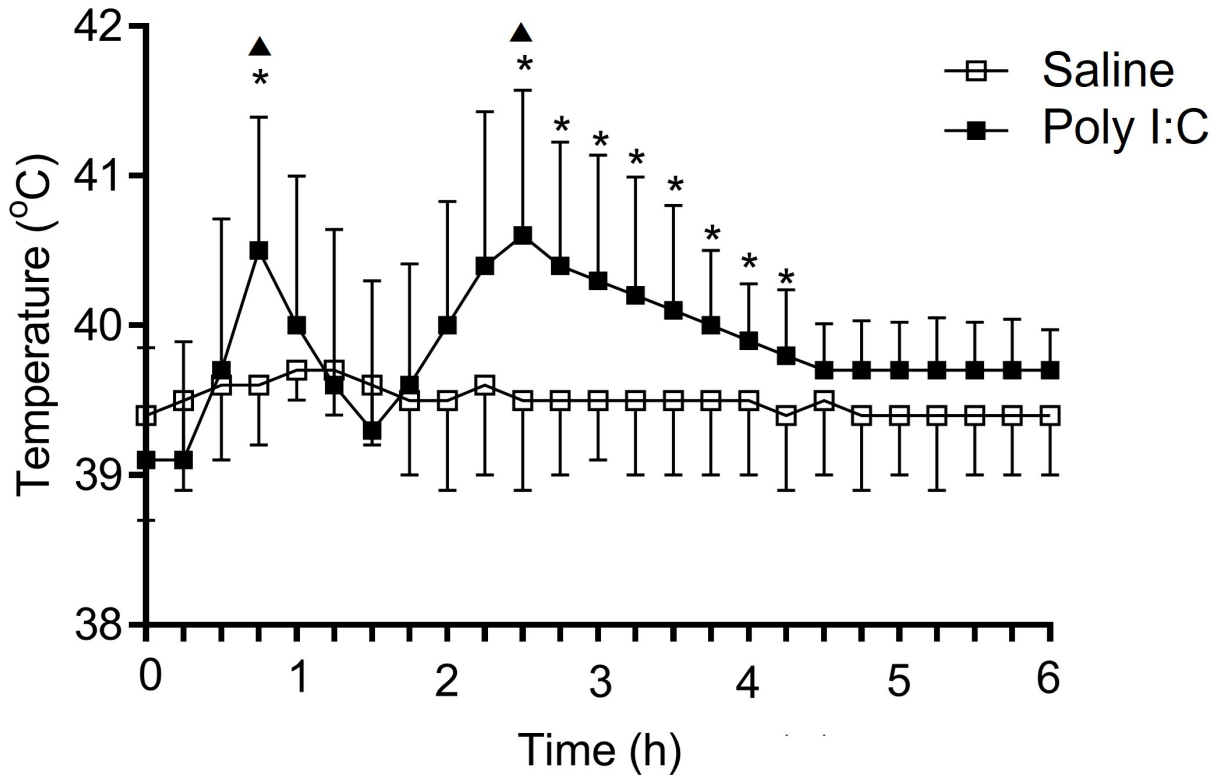
(A) Representative image of the whole brainstem taken with an Axioscanner (AxioScan.Z1scanner, Carl Zeiss, Jena, Germany) showing the location of quantified areas from the rostral ventrolateral areas

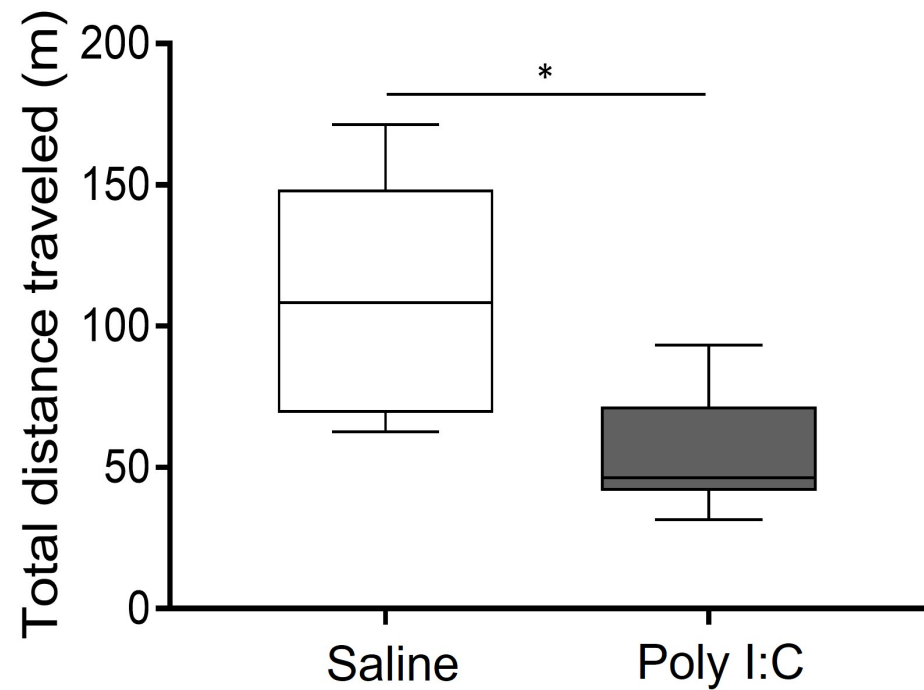
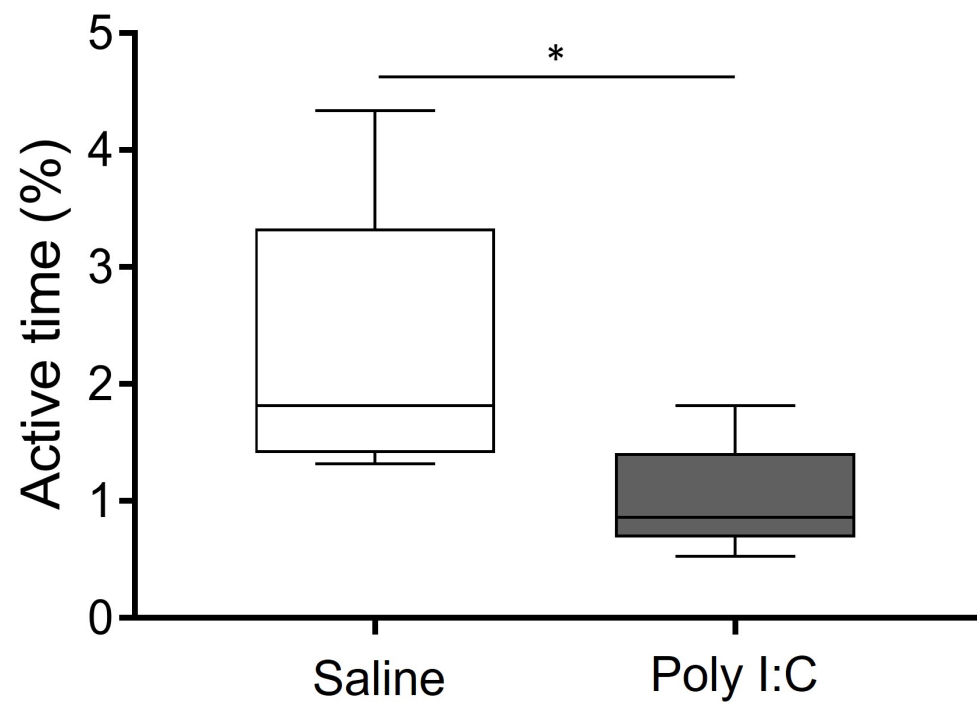
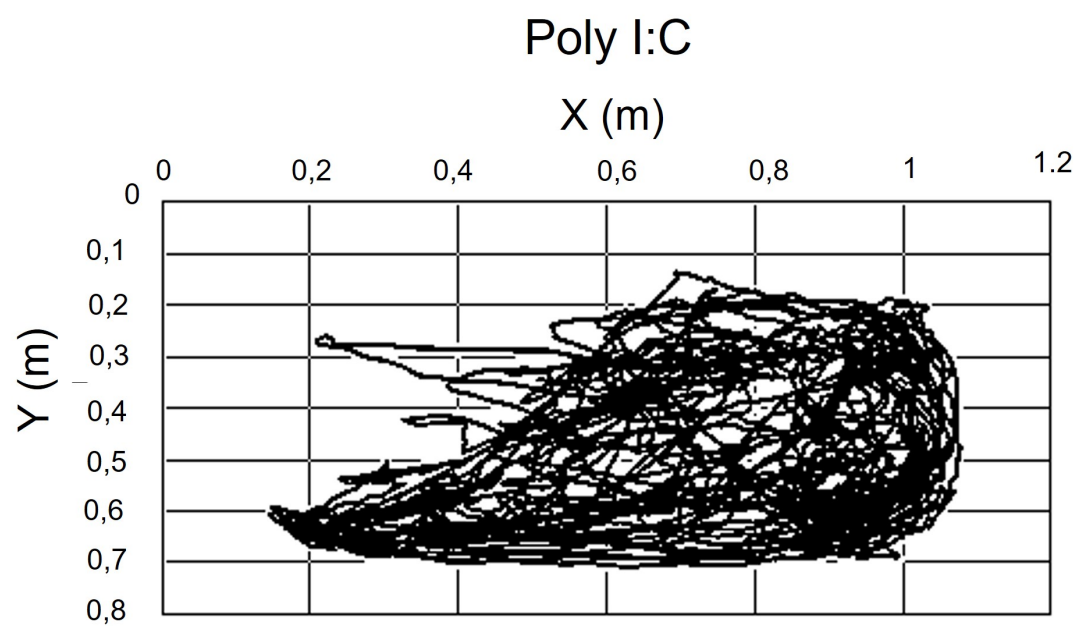
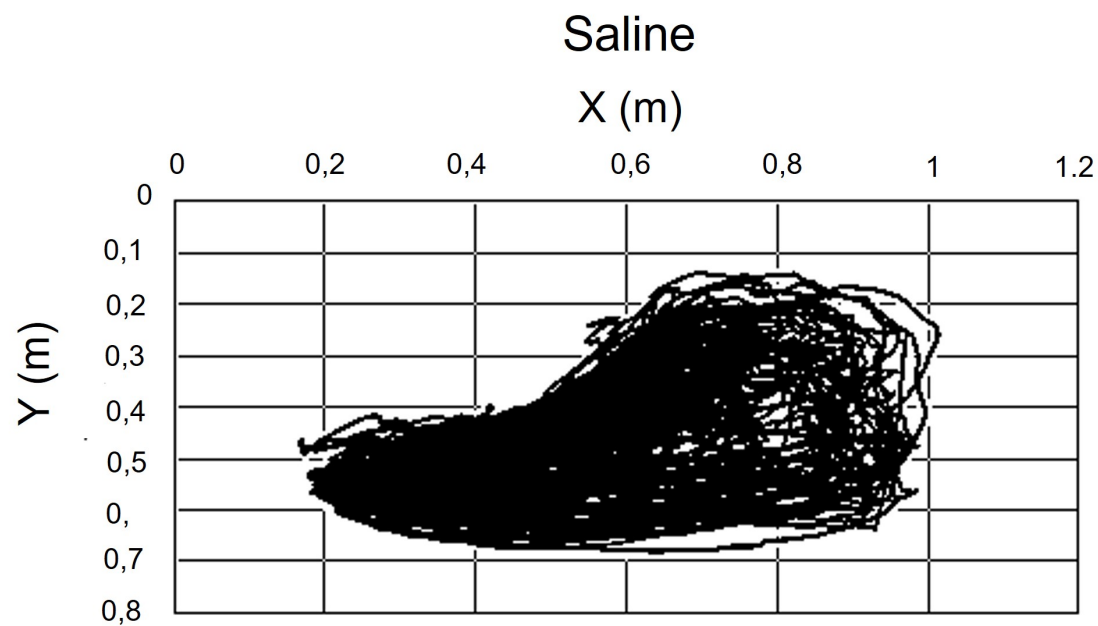
of the medulla (RVLM) and the nucleus tractus solitarius (NTS) in both control and Poly I:C injected lambs.

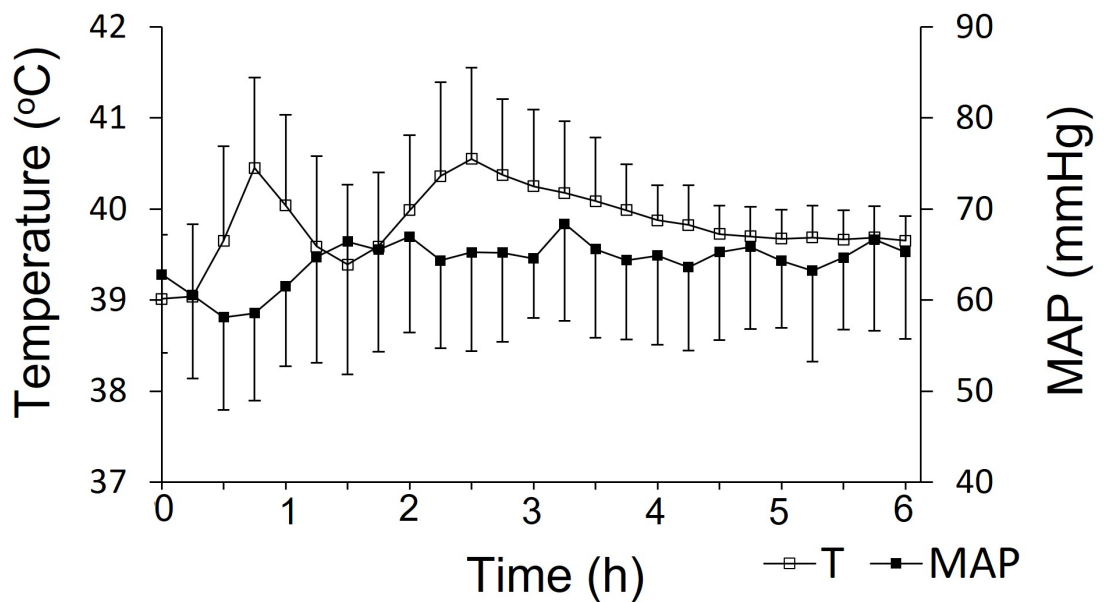
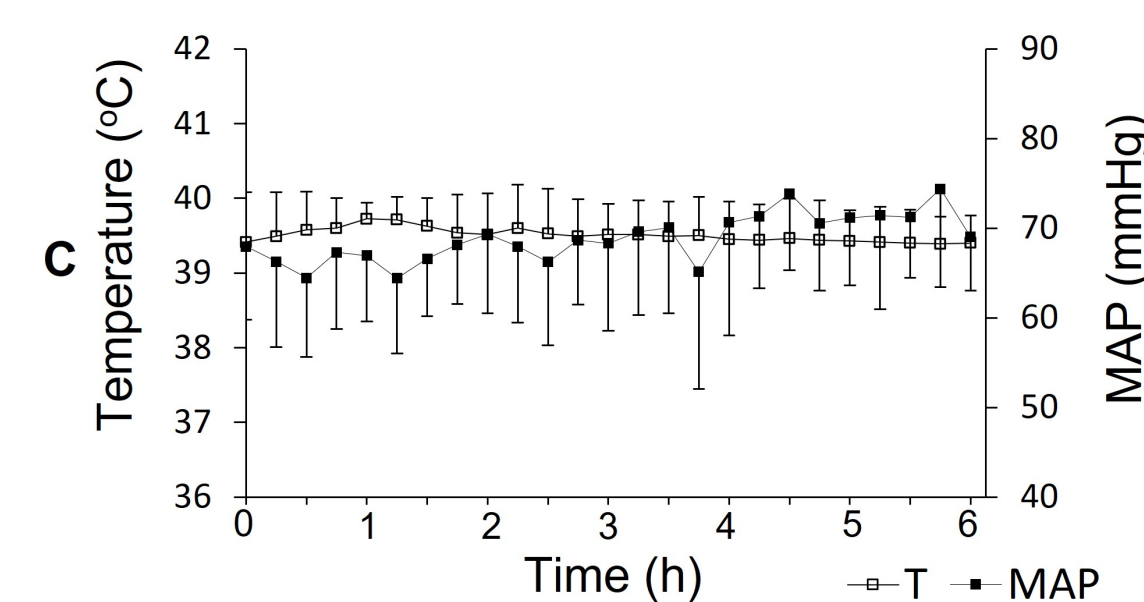
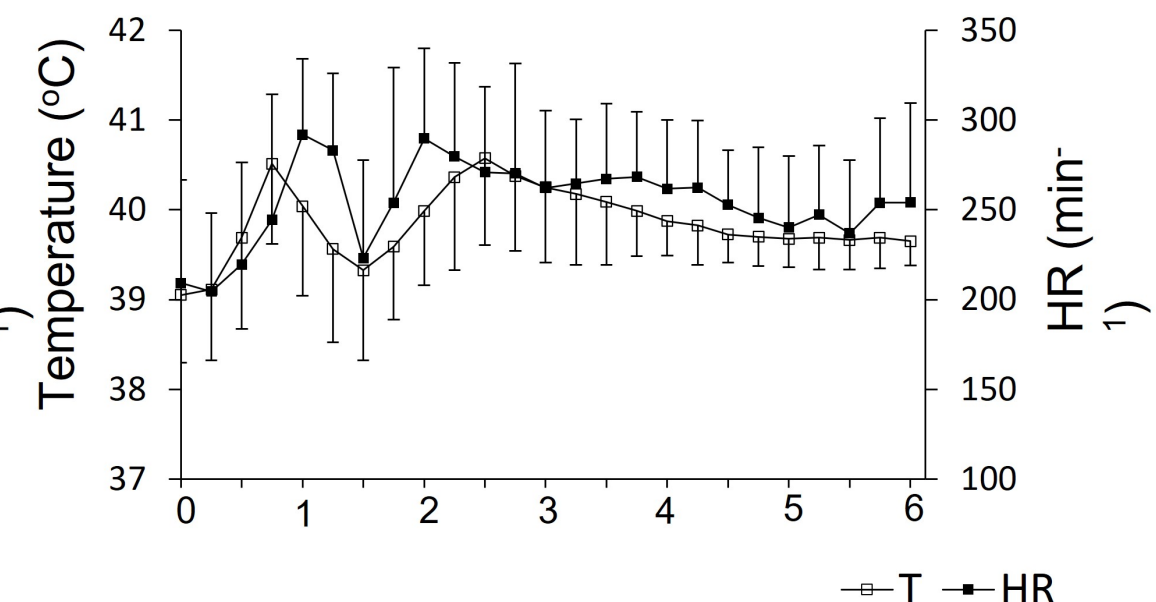
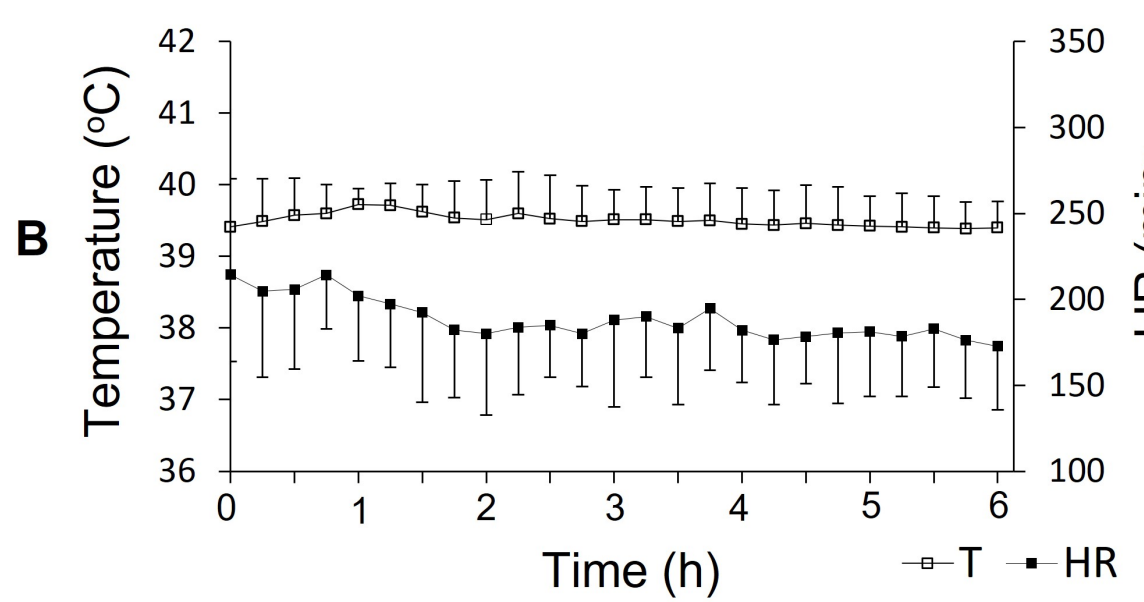
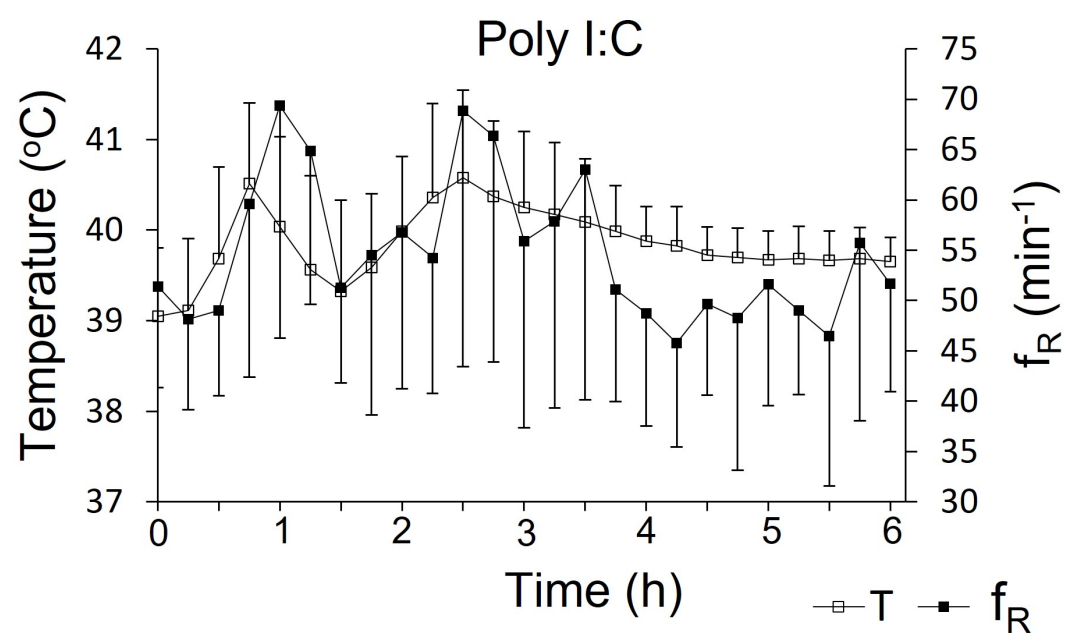
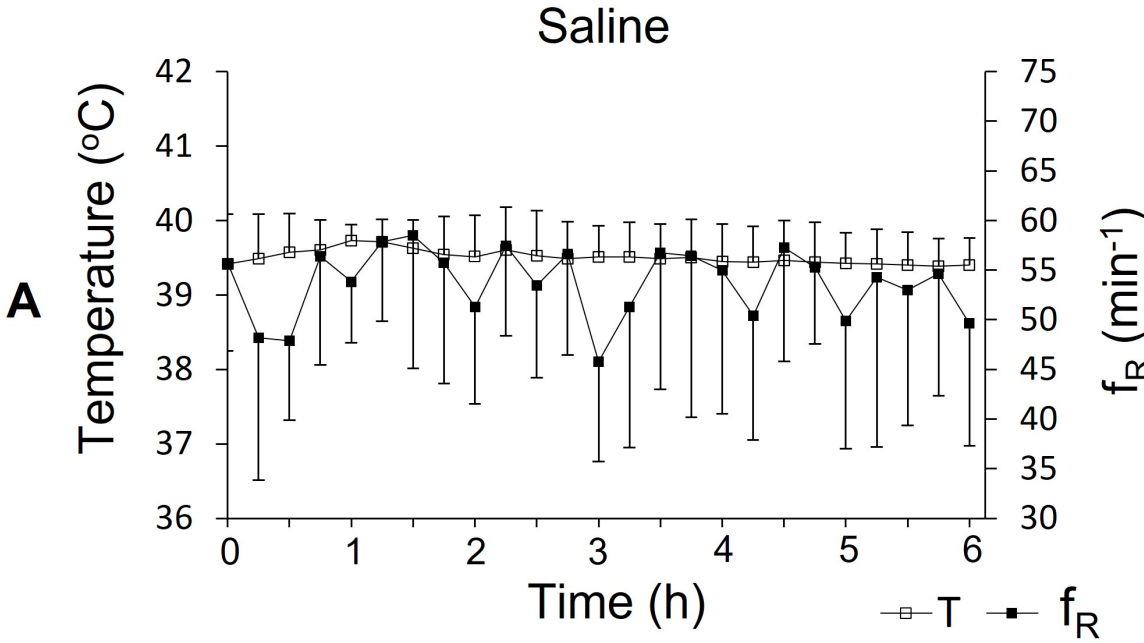
(B-I) 3D confocal stack representative images with full-cell segmentation automatically generated by 3DMorph MATLAB-based script showing how quantitative morphological analysis of microglial cells (Iba1-positive cells in green and GFAP-positive in red) is performed. The full-cell segmentation column shows complete quantified microglial cells remaining after exclusion of partial cells and small processes not related to a cell body. Individual cells were identified, reconstructed, and stained with the colorimetric scale from the largest cell (red) to the smallest (blue).

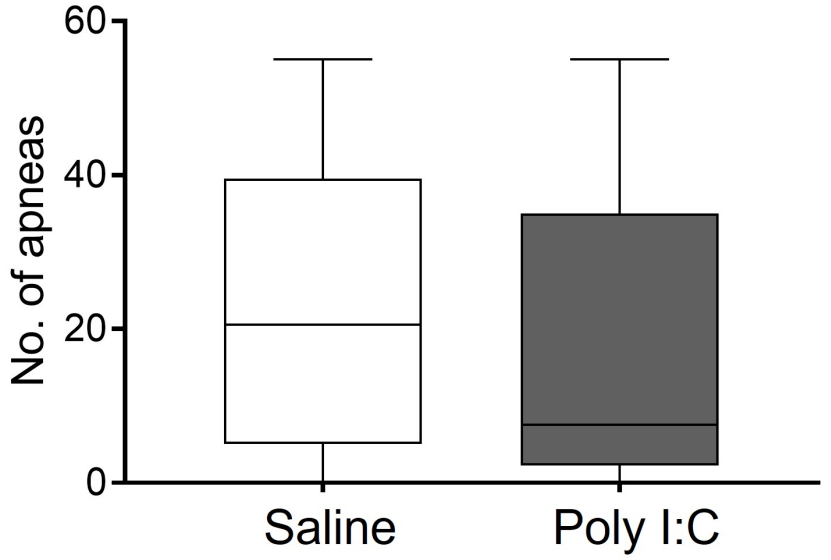
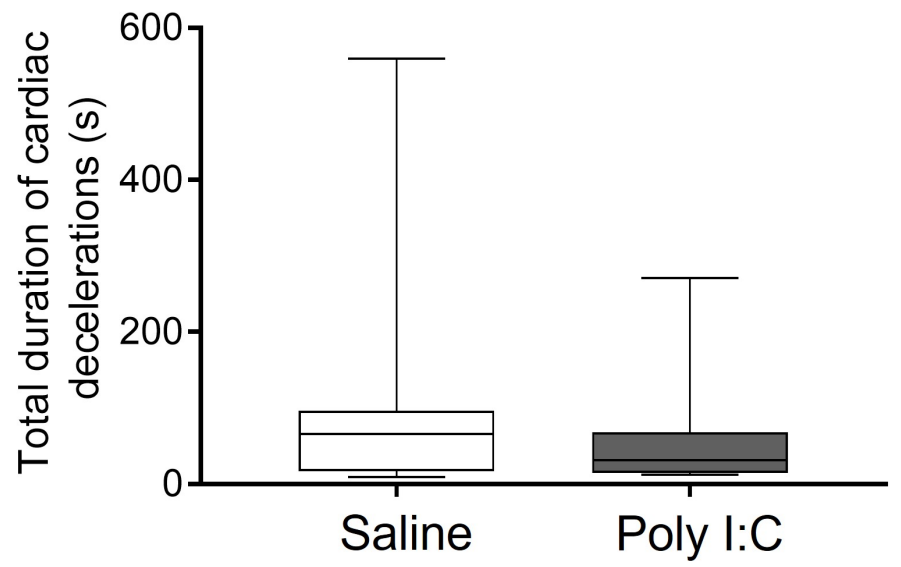
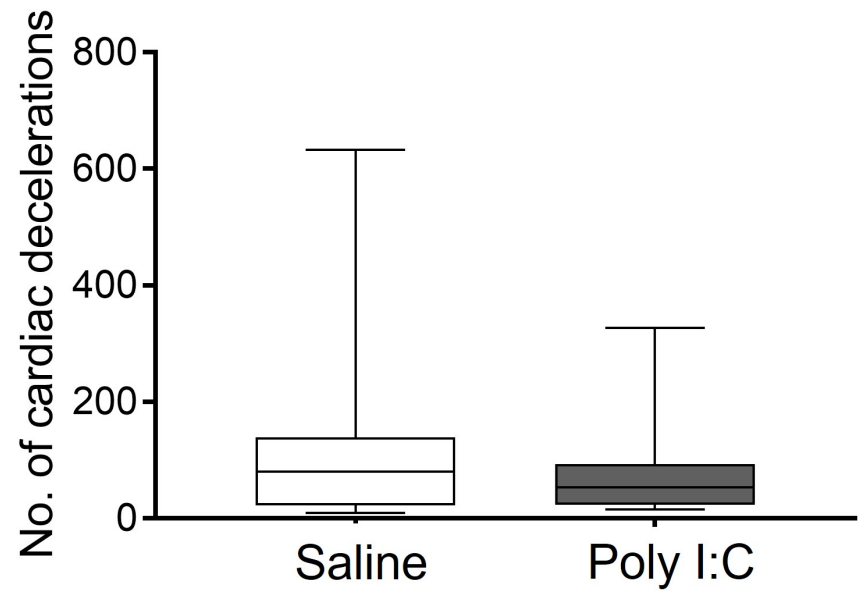
(J-K) Scatter-plot graphs of quantified microglial-cell morphological changes, showing a larger microglial cell-body volume and a larger total territory occupied by microglial cells in Poly I:C-injected lambs compared to controls. Results are presented as median (first and third quartiles), $n = 4$ lambs per group, $n = 35\text{--}65$ cells per group per area.

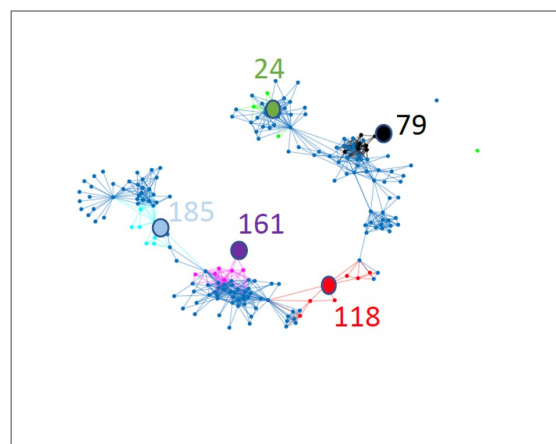
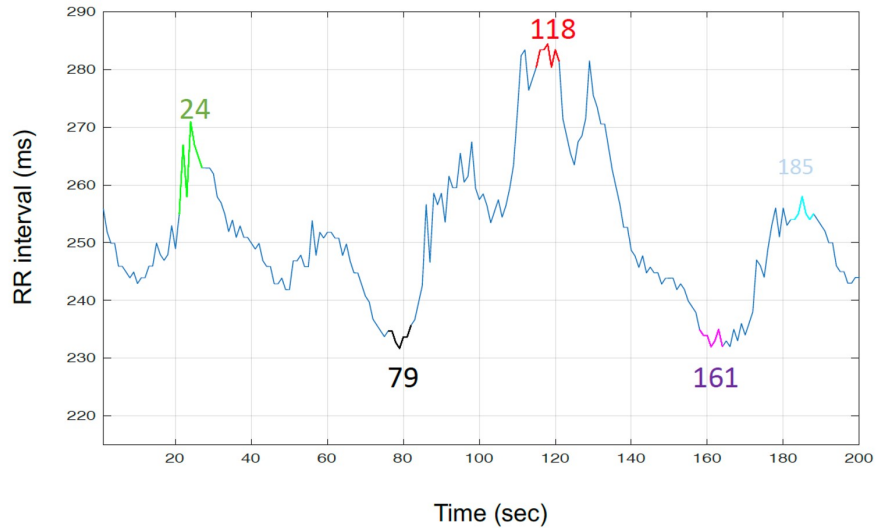
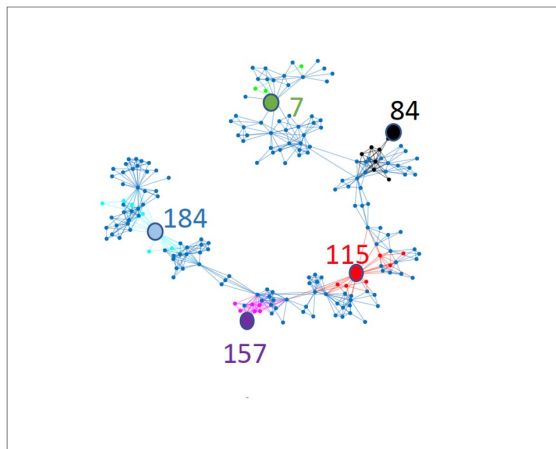
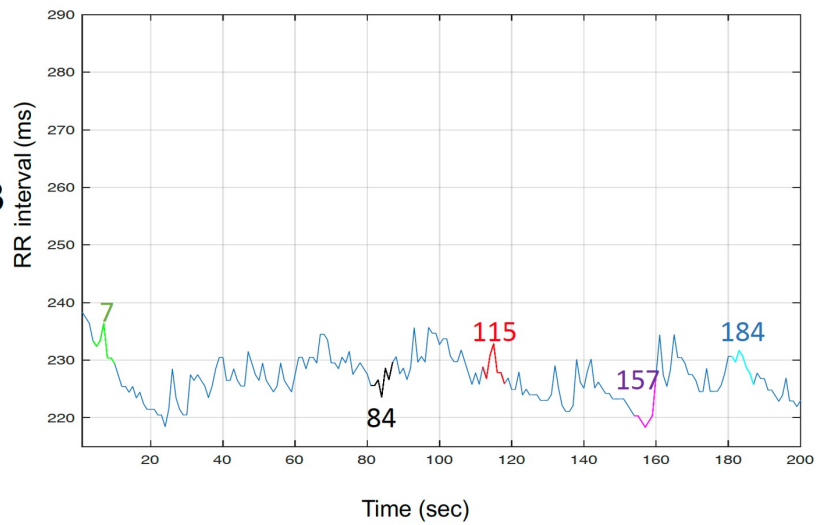
(L) Increased IL-6, IL-8, TNF- α , and Caspase 3 mRNA expression showed by qRT-PCR in the medulla oblongata of Poly I:C-injected lambs compared to controls. Results are expressed as fold increase relatively to an endogenous control (the housekeeping gene SDHA) and presented as mean \pm SEM ($n = 4$ lambs per group). * $P < 0,05$; ** $P < 0,01$; *** $P < 0,001$. Scale bar: 1000 μm in (A); 30 μm in (B, C, F, G).

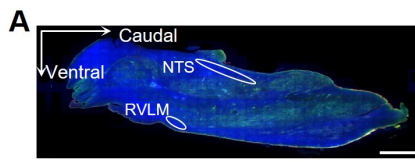


A**B****C**



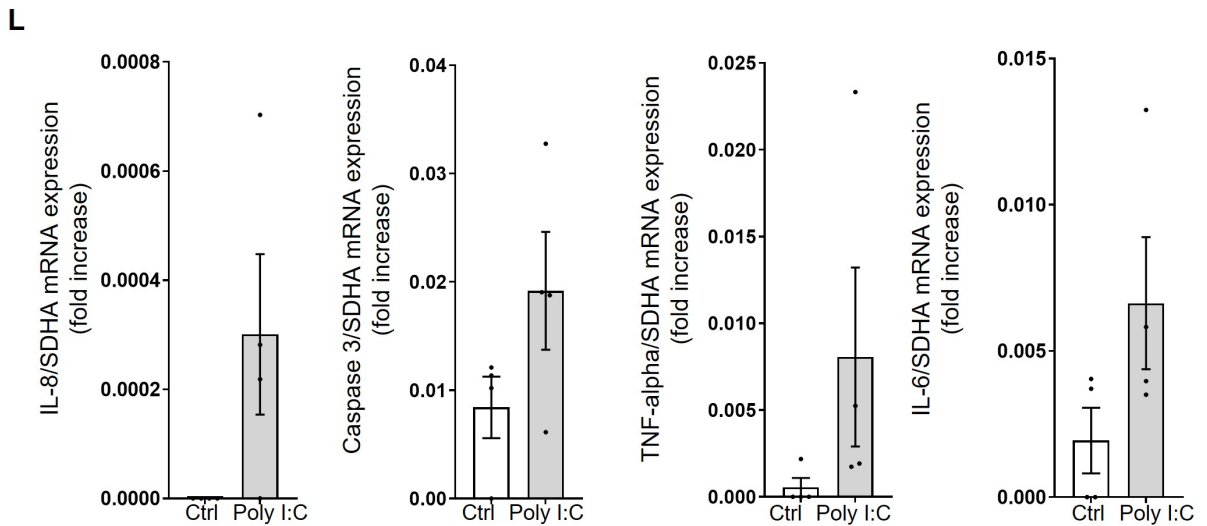
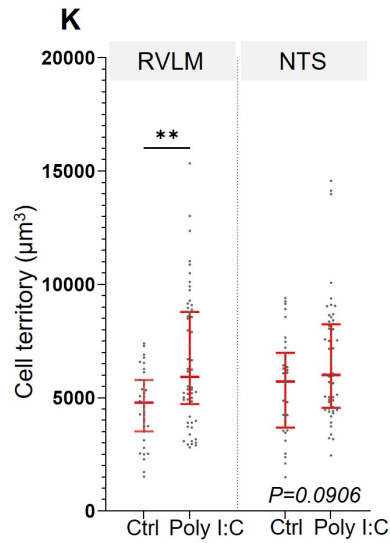
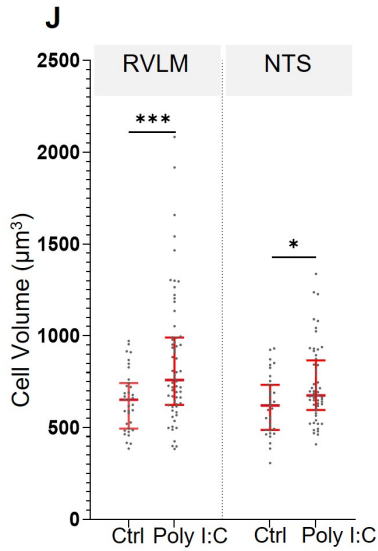
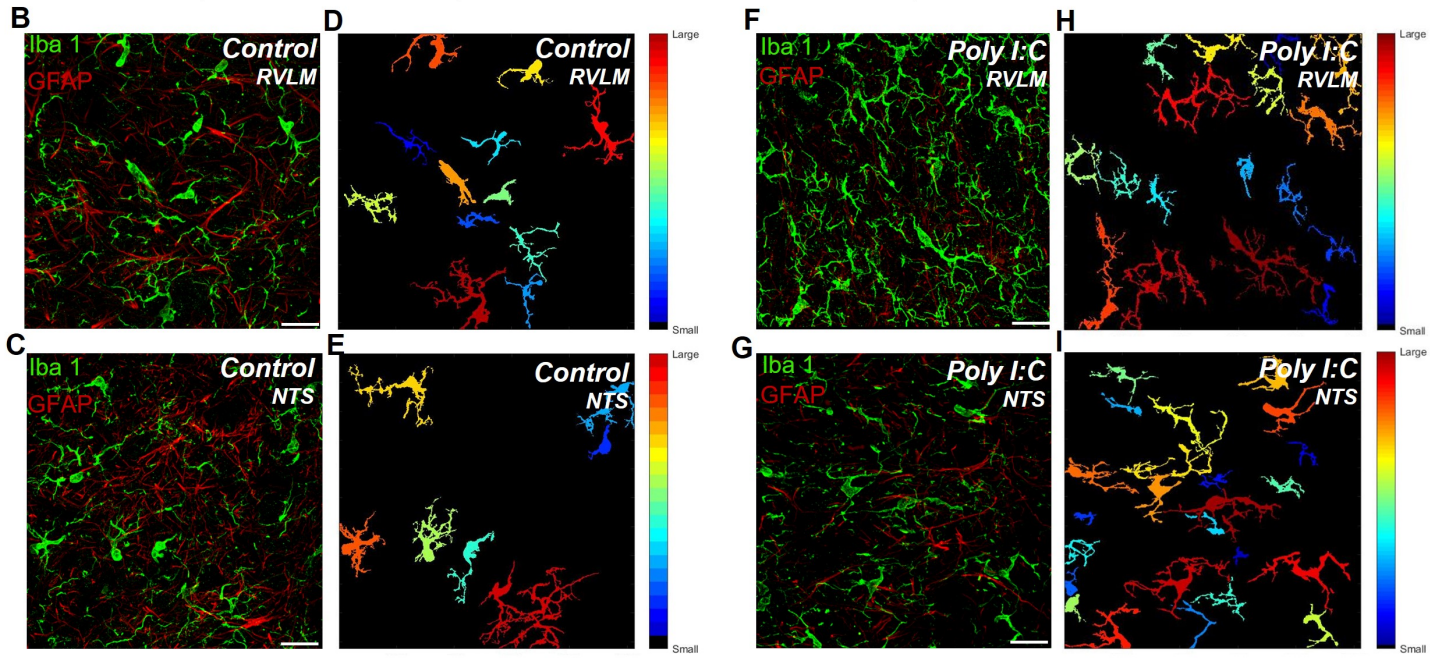
A**B**

A**B**



Control group

Poly I:C group



TABLES

Table 1. Arterial blood gases for each condition.

Results are presented as median (Q1, Q3) at time 0 (T = 0), 3 hours (T = 3) and 6 hours (T = 6) after Poly I:C injection. PaO₂, partial pressure of oxygen in arterial blood; PaCO₂, partial pressure of carbon dioxide in arterial blood; HCO₃⁻, bicarbonate concentration in arterial blood. **p* < 0.05 vs. saline condition.

	T = 0	T = 3	T = 6	T = 0	T = 3	T = 6
	Saline n = 7			Poly I:C n = 7		
PaO ₂ (mmHg)	91 (80, 99)	71 (58, 103)	97 (87, 99)	88 (80, 89)	91 (87, 100)*	92 (86, 96)
PaCO ₂ (mmHg)	38 (33, 40)	40 (39, 40)	38 (34, 43)	35 (28, 39)	36 (33, 37)	35 (34, 39)
pH	7.45 (7.41, 7.48)	7.44 (7.43, 7.45)	7.47 (7.46, 7.49)	7.45 (7.42, 7.47)	7.44 (7.43, 7.50)	7.47 (7.46, 7.50)
HCO ₃ ⁻ (mmol/L)	24 (23, 29)	21 (21, 26)	24 (24, 26)	24 (23, 25)	25 (25, 26)	27 (26, 30)

Table 2. Heart-rate and respiratory-rate variability observed in stationary conditions

n = 8	Saline	Poly I:C at max	p value vs. CTRL
RR (ms)	324 (289, 427)	223 (211, 247)	< 10 ⁻⁶ **
Ttot (ms)	1160 (1040, 1380)	1140 (1010, 1490)	NS
Ti (ms)	540 (490, 600)	530 (470, 630)	NS
Te (ms)	620 (510, 780)	640 (540, 830)	NS
Ti/Ttot	0.46 (0.44, 0.47)	0.46 (0.44, 0.49)	NS
HRV			
SD (ms)	12 (9, 16)	10 (6, 13)	< 10 ⁻⁴
rMSSD (ms)	5 (2, 8)	2 (1, 7)	NS
SD1 (ms)	6 (4, 9)	3 (2, 5)	< 10 ⁻⁶ *
SD2 (ms)	15 (11, 21)	14 (8, 18)	NS
HF (10 ³ • ms ²)	14.28 (7.4, 32.4)	5.45 (1.37, 17.24)	< 10 ⁻³
LF (10 ³ • ms ²)	29.7 (18.5, 59.5)	24.7 (10.5, 41.1)	NS
LF/HF	2.15 (1.44, 3.61)	3.3 (1.8, 5.86)	< 10 ⁻³
SampEn	0.11 (0.03, 0.21)	0.15 (0.07, 0.42)	< 10 ⁻⁴ *
AC	0.38 (0.2, 0.62)	0.26 (0.06, 0.57)	NS
DC	0.46 (0.29, 0.78)	0.39 (0.16, 0.99)	NS
α 1	1.07 (0.97, 1.23)	1.2 (1.07, 1.35)	NS
V-MD	4.74 (4.57, 5.09)	5.59 (4.61, 5.75)	< 10 ⁻³
V-assortativity	0.05 (- 0.04, 0.06)	- 0.04 (- 0.07, 0.01)	< 10 ⁻⁴
V-transitivity	0.44 (0.43, 0.44)	0.42 (0.4, 0.43)	NS
H-MD	2.32 (2.32, 2.32)	2.32 (2.32, 2.32)	NS
H-assortativity	0.09 (0.01, 0.11)	0.01 (- 0.01, 0.06)	< 10 ⁻⁵ *
H-transitivity	0.38 (0.36, 0.4)	0.37 (0.36, 0.38)	< 10 ⁻⁶ *
RRV			
SD Ttot (ms)	120 (90, 160)	150 (110, 210)	NS
SD1 Ttot (ms)	90 (70, 120)	120 (90, 150)	NS
SD2 Ttot (ms)	140 (100, 190)	160 (120, 250)	NS
SampEn Ttot	2.35 (2.21, 2.68)	2.6 (2.31, 3.22)	NS
Cardiorespiratory interrelations			
r ²	0.03 (0.01, 0.07)	0.02 (0.01, 0.06)	NS
h ²	0.07 (0.05, 0.13)	0.06 (0.04, 0.1)	NS
$\gamma_{RR,RESP}$ (n.u.)	0.1 (0.06, 0.13)	0.1 (0.05, 0.13)	NS
RSA (ms)	11.3 (7, 15.7)	5.9 (2.9, 13)	< 10 ⁻⁴

Results are expressed as median (Q1, Q3). The comparisons were made using the first maximum values of changes in heart rate studied in stationary conditions. These maximum values (Poly I:C at max) were obtained between 130 and 260 minutes after injection, corresponding to the 2-hour interval when HR increased above + 3 SD of the control HR. All the available 2-minute stationary intervals collected during this period were used to compute the results. The median number of 2-minute stationary intervals per lamb was 53 (29, 71) in the saline condition and 14 (11,17) in the Poly I:C condition.

RR: cardiac-cycle length; Ttot: respiratory-cycle duration; Ti: inspiratory time; Te: expiratory time; SD: standard deviation; rMSSD: square root of the mean squared differences of successive RR intervals; SD1: Poincaré plot short-term variability coefficient; SD2: Poincaré plot long-term variability coefficient; HF: high frequency; LF: low frequency; SampEn: sample entropy; AC and DC: acceleration and deceleration capacities; α_1 : α_1 fractal coefficient (detrended fluctuation analysis)]; r^2 : Pearson's r^2 correlation coefficient; h^2 : nonlinear h^2 correlation coefficient; $\gamma_{RR,RESP}$: synchronization index; and RSA: amplitude of respiratory sinus arrhythmia.

The new variables used to describe vertical and horizontal visibility are the clustering coefficients V-MD (vertical mean degree) and H-MD (horizontal mean degree)], the assortativity (V-assortativity and H-assortativity), and the transitivity (V-transitivity and H-transitivity)

*: $p < 0.05$ for all lambs except one; **: $p < 0.05$ for all lambs.

SUPPLEMENTAL DATA

Preliminary studies on brainstem inflammation

The methods used in this study for assessing brainstem inflammation, as well as heart-rate and respiratory-rate variability, have been detailed previously¹ and are only summarized herein. Preliminary studies on brainstem inflammation were performed on all eight Poly I:C lambs, six hours after Poly I:C injection, and on eight additional control lambs. Both the Poly I:C and the control group were randomly divided in two subgroups of 4 lambs, for real-time quantitative PCR or for histological studies.

Real-Time quantitative PCR. Following infusion with cold phosphate-buffered saline (PBS) (X1), half of the brainstem was put in a TRIzol solution at – 80 °C. The RNeasy Midi Kit (Qiagen, Mississauga, ON, Canada) was then used to extract total RNA. A Nanodrot 1000 (ThermoFisher Scientific, Waltham, MA, USA) and an Agilent 4200 TapeStation (Agilent, Mississauga, ON, Canada) were utilized to measure RNA concentration and quality respectively. Thereafter, 1µg of total RNA was reverse transcribed using the QuantiTect® Reverse Transcription Kit (Qiagen), and quantitative PCR amplification was conducted for 40 cycles with the QuantStudio™ 6 Flex Real-Time PCR System (Applied Biosystems, Foster City, CA, USA). Briefly, using the appropriate primers (Table S1) and a negative water control for each primer, the amplification of IL-6, IL-8, caspase 3 and TNF-alpha was performed in triplicate. The relative quantification was normalized with the SDHA housekeeping gene as an endogenous control (see details in ¹).

Immunofluorescent staining. The brainstems were fixed in 10% formalin solution, then embedded in OCT (optimum cutting temperature compound) and frozen at -80°C. A

Cryostat Thermo CryoStar NX50 (Thermo Fisher Scientific) was used to perform serial sagittal sections 16 μm thick from the medial to the lateral brainstem. The sections were then incubated with a blocking solution containing 10% normal goat serum, 0.3% bovine serum albumin, and 0.4% TritonX-100 for 30 minutes at room temperature. Subsequently, they were incubated first with the mouse monoclonal anti-GFAP (1/200) (New England Biolabs, Beverly, MA, USA) and rabbit polyclonal anti-Iba1 (1/400) (Wako, Richmond, VA, USA) primary antibodies, then with the goat anti-mouse IgG AlexaFluor 594 (1:500) (Life Technologies, Waltham, MA, USA) and the goat anti-rabbit IgG AlexaFluor 488 (1:200) secondary antibodies.

Analysis of microglial cells. The results from a total of twelve images per region per lamb (four sections \times three images per section) were compared. Iba1-positive cells (microglia) of the rostral ventrolateral medulla and the nucleus tractus solitarius were imaged using confocal microscopy (Leica TCS SP8, Deerfield, IL, USA). Following preprocessing with ImageJ (<https://imagej.net/>), the 3DMorph Automatic Analysis Software (MathWorks, Natick, MA, USA) was used to obtain individual cell volume and total territorial volume of microglial cells².

Heart-rate and respiratory-rate variability

Our previously developed semiautomated processing approach was applied on the ECG and respiratory signals³. Following automatic extraction of all the 2-minute stationary periods⁴ from each 6-hour recording, QRS complexes were automatically detected.

Thereafter, the quality of each RR (cardiac-cycle length) series obtained was checked visually and corrected when necessary.

Heart-rate variability. We selected the following analysis methods of RR interval time series based on past results on neonatal sepsis⁵. For the time-domain analyses, we computed the mean and standard deviation (SD) of RR duration—an index of global HRV—, and the square root of the mean squared differences of successive RR intervals (rMSSD, mainly reflecting parasympathetic control). We computed the sample entropy (SampEn) to assess the complexity and regularity of the RR series. For the frequency-domain analyses, we performed an autoregressive estimation of the power spectrum and integration of the low-frequency (LF, 0.02–0.25 Hz, modulated by the arterial baroreflex) and high-frequency (HF, 0.25–2 Hz, from respiratory origin) spectral bands on the RR series, resampled at 4 Hz⁶. We calculated the LF/HF ratio, an index of sympathovagal balance. In addition, we performed the following nonlinear analyses. We further assessed the short-term (SD1) and long-term (SD2) HRV using the Poincaré plot. We computed the acceleration capacity (AC) and deceleration capacity (DC) as previously described⁵. We tested the scale invariance (self-similarity of RR time series) with the detrended fluctuation analysis technique, using the fractal scaling exponent α ⁷.

In addition, we used new HRV analyses based on the network representations of the horizontal and vertical visibility to further improve the early detection of LOS⁸⁻¹⁰. Using such analyses, the periodicity, fractality, and discontinuity properties of RR time series can be simultaneously assessed, hence providing novel global insight into HRV. The resulting dimensionless network representations (see Supplementary Material,

paragraph entitled “A simple introduction to horizontal and vertical visibility graphs” for a simplified, step-by-step explanation in ¹) reflect the organization of connectivity between the successive RR durations and can differentiate stochastic, chaotic, and deterministic dynamical systems. Alterations in network representations can be visually identified and quantified by calculating the mean degree, assortativity, and transitivity¹¹.

Respiratory-rate variability. Respiratory-rate variability results from the central respiratory drive, which is modulated by multiple nervous and chemical factors, as well as external stimuli. As previously reported³, for the time-domain analyses of RRV on Ttot series, we computed mean and SD. For the nonlinear analyses of RRV, we computed SD1 and SD2 of the Poincaré plots and the sample entropy (SampEn)¹.

Cardiorespiratory interrelations. As previously detailed³, we calculated the Pearson r^2 and the nonlinear h_2 correlation coefficients, the mean phase coherence $\gamma_{RR,RESP}$, and the amplitude of the respiratory sinus arrhythmia¹².

REFERENCES

- 1- Nault, S., Creuze, V., Al-Omar, S., Levasseur, A., Nadeau, C., et al. Cardiorespiratory Alterations in a Newborn Ovine Model of Systemic Inflammation Induced by Lipopolysaccharide Injection. *Front. Physiol.* **11**, 585 (2020).
- 2- York, E.M., LeDue, J.M., Bernier, L.P., MacVicar, B.A. 3DMorph Automatic Analysis of Microglial Morphology in Three Dimensions from Ex Vivo and In Vivo Imaging. *eNeuro* **5**, ENEURO.0266–18.2018–12 (2018).

- 3- Al-Omar, S., Le Rolle, V., Beuchée, A., Samson, N., Praud, J.P., et al. Assessment of tobacco smoke effects on neonatal cardiorespiratory control using a semi-automated processing approach. *Med. Biol. Eng. Comput.* **56**, 2025–2037 (2018).
- 4- Borgnat, P., Flandrin, P., Honeine, P., Richard, C., Xiao, J. Testing stationarity with surrogates: a time-frequency approach. *IEEE. Trans Signal Process.* **58**, 3459–3470 (2010).
- 5- Nguyen, N., Vandenbroucke, L., Hernández, A., Pham, T., Beuchée, A., Pladys, P. Early-onset neonatal sepsis is associated with a high heart rate during automatically selected stationary periods. *Acta Paediatr.* **106**, 749–754 (2017).
- 6- Beuchée, A., Nsegbe, E., St-Hilaire, M., Carrault, G., Branger, B., et al. Prolonged dynamic changes in autonomic heart rate modulation induced by acid laryngeal stimulation in nonsedated lambs. *Neonatology.* **91**, 83–91 (2007).
- 7- Al-Omar, S., Le Rolle, V., Samson, N., Specq, M.L., Bourgoïn-Heck, M., et al Influence of moderate hyperbilirubinemia on cardiorespiratory control in preterm lambs. *Front. Physiol.* **10**, 468 (2019).
- 8- Lacasa, L., Luque, B., Ballesteros, F., Luque, J., Carlos Nuño, J. From time series to complex networks: The visibility graph. *Proc. Natl. Acad. Sci. USA.* **105**, 4972–4975 (2008).
- 9- Madl, T. Network analysis of heart beat intervals using horizontal visibility graphs. 2016 Computing in Cardiology Conference. 733–736 (2016).
- 10- Nguyen Phuc Thu, T., Hernández, A. I., Costet, N., Patural, H., Pichot, V., et al. Improving methodology in heart rate variability analysis for the premature infants: Impact of the time length. *PloS one* **14**, e0220692 (2019).
- 11- Luque, B., Lacasa, L., Ballesteros, F., Luque, J. Horizontal visibility graphs: Exact results for random time series. *Physical Review.* **80**, 046103 (2009).
- 12- Carroll, M.S., Kenny, A.S., Patwari, P.P., Ramirez, J.M., Weese-Mayer, D.E. Respiratory and cardiovascular indicators of autonomic nervous system dysregulation in familial dysautonomia. *Pediatr. Pulmonol.* **47**, 682–691 (2012).

Supplementary Table 1. PCR probes and primers (Invitrogen) used for the study of brainstem inflammation

Gene Symbol	Ref-Seq	Dye-Label	Taqman Assay ID
SDHA	XM_027980212.1	FAM-MGB	Oa04307499_m1
CXCL8	NM_001009401.2	FAM-MGB	Oa04655586_m1
TNF-alpha	NM_001024860.1	FAM-MGB	Oa04656867_g1